J. Math. Biol. (2011) 62:291–331
DOI 10.1007/s00285-010-0332-1

Mathematical Biology

Predator–prey system with strong Allee effect in prey

Jinfeng Wang · Junping Shi · Junjie Wei

Received: 12 June 2009 / Revised: 1 February 2010 / Published online: 12 March 2010

Abstract Global bifurcation analysis of a class of general predator–prey models with a strong Allee effect in prey population is given in details. We show the existence of a point-to-point heteroclinic orbit loop, consider the Hopf bifurcation, and prove the existence/uniqueness and the nonexistence of limit cycle for appropriate range of parameters. For a unique parameter value, a threshold curve separates the overexploitation and coexistence (successful invasion of predator) regions of initial conditions. Our rigorous results justify some recent ecological observations, and practical ecological examples are used to demonstrate our theoretical work.

Keywords Predator–prey model · Allee effect · Global bifurcation · Limit cycles · Heteroclinic loop

This research is supported by the National Natural Science Foundation of China (No 10771045, 10671049) and Program of Excellent Team in HIT, National Science Foundation of US, and Longjiang professorship of Department of Education of Heilongjiang Province.

J. Wang · J. Wei (✉)
Department of Mathematics, Harbin Institute of Technology,
Harbin, 150001 Heilongjiang, People's Republic of China
e-mail: weijj@hit.edu.cn

J. Wang · J. Shi
Y.Y. Tseng Functional Analysis Research Center, Harbin Normal University,
Harbin, 150025 Heilongjiang, People's Republic of China
e-mail: jfwang_math@sohu.com

J. Shi
Department of Mathematics, College of William and Mary,
Williamsburg, VA 23187-8795, USA
e-mail: shij@math.wm.edu

Mathematics Subject Classification (2000) 34C23 · 34C25 · 92D25

1 Introduction

Predator–prey interaction is one of basic interspecies relations for ecological and social models, and it is also the base block of more complicated food chain, food web and biochemical network structure. The first differential equation model of predator–prey type, called Lotka–Volterra equation, was formulated by Lotka (1925) and Volterra (1926) in 1920s, when attempts were first made to find ecological laws of nature. Since then a logistic type growth is usually assumed for the prey species in the models, while a linear mortality rate is assumed for the predator.

Warder Clyde Allee, an American ecologist, asked the question in 1930s (Allee 1931): what minimal numbers are necessary if a species is to maintain itself in nature? In his book, Allee discussed the evidence for the effects of crowding on the demographic and life history traits of populations. Hence the growth rate is not always positive for small density, and it may not be decreasing as in the logistic model either. Generally speaking a population is said to have an Allee effect, if the growth rate per capita is initially an increasing function for the low density. Moreover it is called a strong Allee effect if the per capita growth rate in the limit of low density is negative, and a weak Allee effect means that the per capita growth rate is positive at zero density. A strong Allee effect introduces a population threshold (Courchamp et al. 2008, 1999; Dennis 1989), and the population must surpass this threshold to grow. In contrast, a population with a weak Allee effect does not have a threshold (Courchamp et al. 2008; Dennis 1989; Shi and Shivaji 2006; Wang and Kot 2001). More discussion of definitions can be found in Berec et al. (2007), Courchamp et al. (2008), Gascoigne and Lipcius (2004), Jiang and Shi (2009), and Stephens et al. (1999).

The Allee effect may arise from a number of source such as difficulties in finding mates, reproductive facilitation, predation, environment conditioning and inbreeding depression (Courchamp et al. 2008; Dennis 1989). The Allee effect has been attracting much attention recently owing to its strong potential impact on population dynamics (Berec et al. 2007; Courchamp et al. 2008; Owen and Lewis 2001; Petrovskii et al. 2002; Shi and Shivaji 2006; Wang and Kot 2001). It is widely accepted that the Allee effect may increase the extinction risk of low-density populations (Dennis 1989; Lande 1987). Therefore the population ecology investigation of the Allee effect is important to conservation biology (Burgman et al. 1993; Courchamp et al. 2008; Stephens and Sutherland 1999).

A prototypical predator–prey interaction model is of form

$$\begin{cases} \frac{dX}{ds} = XQ(X) - c_1\phi(X)Y, \\ \frac{dY}{ds} = -d_2Y + c_2\phi(X)Y, \end{cases} \tag{1.1}$$

where the prey X has a growth rate per capita $Q(X)$; d_2 is the death rate of predator; c_1 and c_2 measure the interaction rate of prey and predator, usually $c_1 = 1$ and $c_2 < 1$ is the conversion efficiency; the function $\phi(X)$ is the functional response of

the predator, which corresponds to the saturation of their appetites and reproductive capacity. Usually $\phi(X)$ satisfies that

$$\phi(0) = 0,\ \phi(X) \text{ is increasing},\ \phi(X) \to N \text{ for some } N > 0 \text{ as } X \to \infty.$$

Some conventional functional response functions satisfying these conditions are: (see Holling 1959; Ivlev 1955; Kazarinov and van den Driessche 1978; Turchin 2003)

$$\text{Holling type I}: \ \phi(X) = NX/M,\ 0 \le X \le M,\ \phi(X) = N,\ X > M,\ (M, N > 0);$$

$$\text{Holling type II}: \ \phi(X) = \frac{NX}{A + X};$$

$$\text{Holling type III}: \ \phi(X) = \frac{NX^p}{A^p + X^p},\ (A, N > 0, p > 1);$$

$$\text{Ivlev type}: \ \phi(X) = N - e^{-AX},$$

and more can be found in for example (Turchin 2003). When $Q(X)$ is of a logistic growth, the dynamics of (1.1) has been considered in many articles, see for example (Cheng 1981; Hsu 1978; Hsu and Shi 2009; Kuang and Freedman 1988; May 1972; Rosenzweig 1971; Xiao and Zhang 2003), and many more investigations in recent years. For (1.1) with logistic growth on the prey and Holling II type functional response (known as Rosenzweig–MacArthur model 1963), a complete dynamical analysis can be obtained (see Albrecht et al. 1973, 1974; Cheng 1981; Hsu and Shi 2009; Kuang and Freedman 1988; May 1972; Rosenzweig 1971). When fixing other system parameters but change the carrying capacity of the prey from small to large, first the prey-only equilibrium loses the (global) stability to a globally stable coexistence equilibrium, then with the carrying capacity going further large, a unique limit cycle which is globally asymptotically orbital stable arises from a Hopf bifurcation. These mathematical results provide important information for the ecological studies (May 1972; Rosenzweig 1971; Rosenzweig and MacArthur 1963).

In this paper, we rigorously consider the global dynamics of (1.1) with an increasing and bounded functional response, and the prey satisfies a strong Allee effect growth. In fact we study a predator–prey system under very general conditions:

$$\begin{cases} \frac{du}{dt} = g(u)(f(u) - v), \\ \frac{dv}{dt} = v(g(u) - d), \end{cases} \tag{1.2}$$

where f, g satisfy: (here $\mathbb{R} = (0, \infty)$)

(a1) $f \in C^1(\overline{\mathbb{R}^+})$, $f(b) = f(1) = 0$, where $0 < b < 1$; $f(u)$ is positive for $b < u < 1$, and $f(u)$ is negative otherwise; there exists $\bar{\lambda} \in (b, 1)$ such that $f'(u) > 0$ on $[b, \bar{\lambda})$, $f'(u) < 0$ on $(\bar{\lambda}, 1]$;

(a2) $g \in C^1(\overline{\mathbb{R}^+})$, $g(0) = 0$; $g(u) > 0$ for $u > 0$ and $g'(u) > 0$ for $u > 0$, and there exists $\lambda > 0$ such that $g(\lambda) = d$.

Here $g(u)$ is the predator functional response, and $g(u)f(u)$ is the net growth rate of the prey. The graph of $v = f(u)$ is the prey nullcline on the phase portrait. In the

absence of the predator, the prey u has a strong Allee effect growth which is reflected from the assumptions (a1). The carrying capacity of the prey is rescaled into 1 here, while b is the survival threshold or sparsity constant of the prey. The predator nullcline is a vertical line $u = \lambda$ solved from $g(\lambda) = d$. The condition (a2) on the functional responde $g(u)$ includes the commonly used Holling types I, II and III as well as the linear one ($g(u) = u$ as Lotka–Volterra). The parameter d is the mortality rate of predator; the number λ can also be thought as a measure of the predator mortality as λ increases with d, and λ is also the stationary prey population density coexisting with predator. As pointed out by Bazykin (1998), it is natural to regard λ as a measure of how well the predator is adapted to the prey. In our analysis λ plays a pivotal role as the main bifurcation parameter. The equation (1.2) is a non-dimensionalized version in which the conversion efficiency of prey biomass into predator biomass is rescaled to 1. This does not limit the applicability of our results as all results can be stated in the original system parameters. We use the non-dimensionalized equation to simplify our presentation. On the other hand, we note that non-monotonic functional responses like Holling type IV or Monod–Haldane function: $g(u) = Nu/(u^2 + Au + B)$, $B, N > 0$ and $A \geq 0$, has also been considered in certain situations (Aguirre Pablo et al. 2009; González-Olivares et al. 2006; Ruan and Xiao 2000/01), and our results here do not apply to it. Neither we consider here the predator-dependent functional responses such as ratio-dependent type (Arditi and Ginzburg 1989; Hsu et al. 2001; Kuang and Beretta 1998; Xiao and Ruan 2001). Also in this paper we always assume the Allee effect is strong, although some techniques can be used for weak Allee effect case as well (which we will report in another paper).

Earlier analytic work on special cases of (1.2) appeared in Bazykin (1998) Sect. 3.5.5 and Conway and Smoller (1986), and they considered the Lotka–Volterra case $g(u) = u$. A more recent analysis of (1.2) with $g(u) = mu/(a+u)$ has been done by Malchow et al. (2008) see Sect. 12.1. The invasion mechanism of scalar reaction-diffusion model with strong Allee effect was considered in Lewis and Kareiva (1993). The system (1.2) in the context of reaction-diffusion models was first proposed in Owen and Lewis (2001), and also Petrovskii et al. (2002). Also the dynamical properties of some special cases of system (1.2) have been obtained by numerical simulation in recent studies (Boukal et al. 2007; Lande 1987; Malchow et al. 2008; van Voorn et al. 2007; Wang and Kot 2001). Our analysis here is rigorous and our assumptions on the model appear to be general enough to cover most of previous investigations. Our results depend neither on the specific algebraic forms of the growth rates and functional response, nor on specific parameterizations. We provide theoretical analysis by utilizing planar portrait analysis, performing Hopf bifurcation analysis, and transforming the system into a nonlinear Liénard equation. The results include the existence/uniqueness and nonexistence of limit cycle, and the existence/uniqueness of point-to-point heteroclinic orbit, which coincide with the simulation results (Malchow et al. 2008; van Voorn et al. 2007) and provide vital information for some ecological phenomena (Boukal et al. 2007), especially the explanation of Allee threshold.

The rest of the paper is structured in the following way. In Sect. 2, we carry out the phase plane analysis of (1.2). From stability analysis and properties of the stable manifold and unstable manifold of equilibrium points, we show the existence and uniqueness of a point-to-point heteroclinic orbit loop. In Sect. 3, Hopf bifurcation from

the coexistence equilibrium point is analyzed, and in Sect. 4 we prove the uniqueness and nonexistence of the limit cycle by translating (1.2) into a Liénard equation. Applications to specific predator–prey models and related biological discussions are given in Sect. 5. Some concluding remarks are given in Sect. 6. In Appendix section, technical details of Hopf bifurcation analysis is given.

2 Phase portrait

For (1.2), the positive quadrant of the phase plane $\{(u, v) : u > 0, v > 0\}$ is invariant. The following lemma guarantees that the system (1.2) is dissipative.

Lemma 2.1 *Suppose that f, g satisfy* (a1)–(a2)*. Then any solution of* (1.2) *with positive initial value is positive and bounded.*

Proof The first quadrant is an invariant region for (1.2) since $\{(u, v) : u = 0\}$ and $\{(u, v) : v = 0\}$ are invariant manifolds of (1.2). Therefore the solutions of (1.2) with the initial values $u(0) > 0$ and $v(0) > 0$ are positive. For any $u(0) > 1$, then $u' = g(u)(f(u) - v) < 0$ as long as $u > 1$; along $u = 1$, $u' = -g(1)v < 0$; and there is no any equilibrium point in the region $\{(u, v) : u > 1, v \geq 0\}$. Hence any positive solution satisfies $u(t) \leq \max\{u(0), 1\}$ for $t \geq 0$. Adding the two equations in (1.2), we obtain that $(u + v)' = g(u) f(u) - dv$. Let $\eta = \max_{t \geq 0} (g(u(t)) f(u(t)) + du(t))$. Then we have $(u + v)' \leq \eta - d(u + v)$. From Gronwall's inequality, we obtain that

$$u(t) + v(t) \leq (u(0) + v(0))\, e^{-dt} + \frac{\eta}{d}(1 - e^{-dt}).$$

Hence $v(t)$ is also bounded. □

There are four possible equilibrium points:

$$O = (0, 0),\ A = (1, 0),\ B = (b, 0),\ C = (\lambda, v_\lambda) = (\lambda, f(\lambda)),$$

where λ is defined in (a2) (since $g(u)$ is strictly increasing, then λ is apparently unique). C is the intersection of the prey nullcline $v = f(u)$ and the predator nullcline $g(u) = d$ (or $u = \lambda$), and it is a positive equilibrium only when $b < \lambda < 1$ (see Fig. 1). Otherwise there are only three equilibrium points in the positive quadrant or on the boundary. We point out that when $0 < \lambda \leq b$, the dynamics is trivial that the extinction equilibrium point $O = (0, 0)$ is globally asymptotically stable for all initial value (u_0, v_0) with $u_0 > 0$ and $v_0 > 0$; and when $\lambda \geq 1$, the attraction basins of two locally stable equilibrium points $O = (0, 0)$ and $A = (1, 0)$ split the first quadrant. See Theorem 2.6 for details. Hence we concentrate on the case of $b < \lambda < 1$ below.

The Jacobian matrix of (1.2) is

$$J = \begin{pmatrix} g'(u)(f(u) - v) + g(u) f'(u) & -g(u) \\ g'(u)v & g(u) - d \end{pmatrix}.$$

Assume $b < \lambda < 1$ (hence the positive equilibrium $O = (\lambda, v_\lambda)$ exists), then for the three boundary equilibrium points, we have the following information:

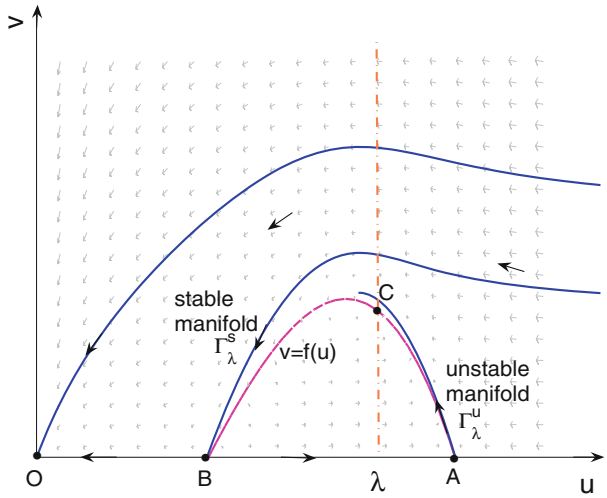

Fig. 1 Basic phase portrait of (1.2) with a coexistence equilibrium point ($b < \lambda < 1$). The *horizontal axis* is the prey population u, and the *vertical axis* is the predator population v. The *dashed curve* is the u-nullcline $v = f(u)$, and the *dashed-dotted vertical line* is the v-nullcline $g(u) = d$ or $u = \lambda$

1. At $(0, 0)$, the eigenvalues of the Jacobian are $\mu_1 = f(0)g'(0) < 0$ and $\mu_2 = -d < 0$, thus $(0, 0)$ is a stable node;
2. At $(b, 0)$, the eigenvalues of the Jacobian are $\mu_1 = g(b)f'(b) > 0$ and $\mu_2 = g(b) - d < 0$, so $(b, 0)$ is a saddle with its unstable manifold along the u axis and its stable manifold (denoted by Γ^s_λ) entering from the region above the prey nullcline $v = f(u)$;
3. At $(1, 0)$, the eigenvalues of the Jacobian are $\mu_1 = g(1)f'(1) < 0$ and $\mu_2 = g(1) - d > 0$, hence $(1, 0)$ is a saddle with its stable manifold along the u axis and its unstable manifold (denoted by Γ^u_λ) entering the region $v > f(u)$.

At the positive equilibrium point (λ, v_λ), the eigenvalues of the Jacobian satisfy $\mu^2 - \mu T + D = 0$, where

$$T := Tr\, J = g(\lambda)f'(\lambda), \tag{2.1}$$

$$D := det\, J = g(\lambda)g'(\lambda)f(\lambda). \tag{2.2}$$

From (a1), $\bar{\lambda}$ is the unique positive root of $T(\lambda) = 0$. When $b < \lambda < \bar{\lambda}$, $T > 0$ and $D > 0$, then (λ, v_λ) is unstable; When $\bar{\lambda} < \lambda < 1$, $T < 0$ and $D > 0$, then (λ, v_λ) is locally stable. We shall use λ as a bifurcation parameter to consider the change of the dynamics of (1.2).

When $b < \lambda < 1$, the separatrices Γ^s_λ and Γ^u_λ are the keys to understand the dynamical behavior of (1.2) (See Fig. 1). First we prove a general property of Γ^s_λ and Γ^u_λ:

Proposition 2.2 *Suppose that $b < \lambda < 1$. Let Γ^s_λ and Γ^u_λ be the stable manifold of $(b, 0)$ and the unstable manifold of $(1, 0)$ respectively. Then*

1. *The orbit* Γ^s_λ *meets the nullcline* $u = \lambda$ *at a point* $(\lambda, S(\lambda))$*, where* $S(\lambda) \geq v_\lambda := f(\lambda)$*, and* $S(\lambda)$ *is a strictly increasing continuous function for* $\lambda \in (b, 1)$.
2. *The orbit* Γ^u_λ *meets the nullcline* $u = \lambda$ *at a point* $(\lambda, U(\lambda))$*, where* $U(\lambda) \geq v_\lambda := f(\lambda)$*, and* $U(\lambda)$ *is a strictly decreasing continuous function for* $\lambda \in (b, 1)$.

Proof The eigenvalues of the Jacobian matrix of (1.2) at B are $\mu_1 = g(b)f'(b) > 0$ and $\mu_2 = g(b) - d < 0$, and the corresponding eigenvector of μ_2 is $\left(\frac{g(b)}{g(b)f'(b)-g(b)+d}, 1\right)^T$. Hence the tangential direction of Γ^s_λ at B is

$$k_1 = \frac{g(b)f'(b) - g(b) + d}{g(b)} = \frac{-g(b) + d}{g(b)} + f'(b),$$

while the tangential direction of the nullcline $v = f(u)$ at B is $k_2 = f'(b)$. Since $d = g(\lambda) > g(b)$, then $k_1 > k_2$. Therefore Γ^s_λ is above the nullcline $v = f(u)$, that is Γ^s_λ approaches B from the region $\{(u, v) : v > f(u)\}$. Moreover from the direction of the vector field in (1.2) on the nullcline $v = f(u)$, Γ^s_λ always remains above $v = f(u)$ for $u < \lambda$.

Hence to show that Γ^s_λ meets the line $u = \lambda$, we need only to show that it remains bounded for $u > b$. Indeed for $u > b$, Γ^s_λ is the graph of a function $v(u)$, and $v(u)$ satisfies

$$\frac{dv(u)}{du} = \frac{v'}{u'} = \frac{v(g(\lambda) - g(u))}{g(u)(v - f(u))}. \tag{2.3}$$

If $v(u) \to \infty$ as $u \to \lambda_a^-$ for some $\lambda_a < \lambda$, then $v - f(u)$ is bounded from below for $b + \varepsilon \leq u \leq \lambda_a$ and any $\varepsilon > 0$, since Γ^s_λ is above $v = f(u)$. Thus for $b + \varepsilon \leq u \leq \lambda_a$,

$$\frac{dv}{du} \leq cv \tag{2.4}$$

for some positive constant c. But (2.4) would imply that $v(u)$ is bounded as $u \to \lambda_a^-$, that is a contradiction. Thus $v(u)$ cannot blow up before it is extended to $u = \lambda$. Therefore $S(\lambda)$ exists for all $\lambda \in (b, 1)$ and $S(\lambda) \geq v_\lambda$. It is also clear that $S(\lambda)$ is a continuous function if $S(\lambda) \neq v_\lambda$.

Note that $S(\lambda) = v_\lambda$ only when $\Gamma^s_\lambda \to C$ as $t \to -\infty$, so in that case, C must be an unstable equilibrium point with real eigenvalues. When $\lambda > \bar{\lambda}$, C is locally stable, thus $S(\lambda) > v_\lambda$ if $\lambda > \bar{\lambda}$. When $\lambda \leq \bar{\lambda}$ and λ is near $\bar{\lambda}$, C is an unstable spiral. Thus the set $\Sigma = \{\lambda \in (b, 1) : S(\lambda) > v_\lambda\}$ is a nonempty open subset containing $(\bar{\lambda} - \varepsilon, 1)$ for some $\varepsilon > 0$.

We show that $S(\lambda)$ is strictly increasing on any component of Σ. Let $\lambda_1 < \lambda_2$ be two points in a connected component of Σ. The stable manifolds at B for λ_1 and λ_2 are graphs of functions $v_1(u)$ and $v_2(u)$ defined for $u > b$ respectively. The eigenvectors at B are respectively

$$x_1 = \left(\frac{g(b)}{g(b)f'(b) - g(b) + g(\lambda_1)}, 1\right)^T, \quad x_2 = \left(\frac{g(b)}{g(b)f'(b) - g(b) + g(\lambda_2)}, 1\right)^T.$$

Hence from comparison arguments, $v_2(u) > v_1(u)$ for u sufficiently near b. Suppose that $v_1(u) = v_2(u)$ for some u with $b < u \leq \lambda_1$. Let $\bar{u}$ be the smallest such value. Then we must have

$$0 \leq v_2'(\bar{u}) \leq v_1'(\bar{u}).$$

But from (2.3) we would have

$$\frac{v_2(\bar{u})(g(\lambda_2) - g(\bar{u}))}{g(\bar{u})(v_2(\bar{u}) - f(\bar{u}))} \leq \frac{v_1(\bar{u})(g(\lambda_1) - g(\bar{u}))}{g(\bar{u})(v_1(\bar{u}) - f(\bar{u}))}. \tag{2.5}$$

However, since $v_2(\bar{u}) = v_1(\bar{u})$, we see that $\lambda_2 \leq \lambda_1$, which is a contradiction. Thus $v_2(\lambda_1) > v_1(\lambda_1) = S(\lambda_1)$, and $S(\lambda_2) > S(\lambda_1)$ as claimed. Notice that the argument above indeed shows that if $\lambda_1 \in \Sigma$ and $S(\lambda_1) > v_\lambda$, then any $\lambda \in (\lambda_1, 1)$ also belongs to Σ and $S(\lambda) > S(\lambda_1)$.

Hence $\Sigma = (\lambda_b, 1)$ for some $\lambda_b \in (b, \bar{\lambda})$. For $\lambda \in (b, \lambda_b]$, $S(\lambda) = v_\lambda$, and for $\lambda \in (\lambda_b, 1)$, $S(\lambda) > v_\lambda$. For both cases, $S(\lambda)$ is increasing since v_λ is increasing for $\lambda < \bar{\lambda}$. This completes the proof of part 1. The proof of part 2 is similar. □

The monotonicity of $S(\lambda)$ and $U(\lambda)$ naturally implies the following result:

Proposition 2.3 *There exists a unique* $\lambda^\sharp \in (b, 1)$*, such that* $\Gamma^s_{\lambda^\sharp} = \Gamma^u_{\lambda^\sharp}$.

Proof Notice that

$$\lim_{\lambda \to b^+} [S(\lambda) - U(\lambda)] < 0, \quad \text{and} \quad \lim_{\lambda \to 1^-} [S(\lambda) - U(\lambda)] > 0.$$

Therefore, from the monotonicity of U and S, there is a unique $\lambda^\sharp$ such that $S(\lambda) = U(\lambda)$. Furthermore, for this $\lambda^\sharp$ we have two distinct saddle-saddle connections, which forms a heteroclinic cycle between A to B (see Fig. 3b). □

$\lambda = \lambda^\sharp$ is clearly a threshold value for the dynamics of (1.2)–it is the only parameter value so that (1.2) possesses a loop of heteroclinic orbits between A and B. Since all solutions are bounded from Lemma 2.1, from the celebrated Poincaré–Bendixson Theorem (see Wiggins (1990) Theorem 1.1.19), only when $\lambda = \lambda^\sharp$, the ω-limit set of a positive orbit of (1.2) can be a loop of heteroclinic orbits, and for $\lambda \neq \lambda^\sharp$, the ω-limit set of a positive orbit must be either an equilibrium point or a periodic orbit. A rough picture of the dynamics can be stated as follows:

Proposition 2.4 *Let* $(u(t), v(t))$ *be the solution of* (1.2) *with positive initial value* (u_0, v_0).

1. *When* $b < \lambda < \lambda^\sharp$, $S(\lambda) < U(\lambda)$, *and* Γ^u_λ *can be expressed as* $\{(u, v^u(u)) : 0 < u < 1\}$ *with* $\lim_{u \to 0^+} v^u(u) = 0$. *If* $u_0 \geq 1$ *or* $0 < u_0 < 1$ *and* $v_0 \geq v^u(u_0)$, *then* $(u(t), v(t)) \to (0, 0)$ *as* $t \to \infty$; *if* $0 < u_0 < 1$ *and* $0 < v_0 < v^u(u_0)$, *then either* $(u(t), v(t)) \to (\lambda, v_\lambda)$, $(0, 0)$ *or a periodic orbit as* $t \to \infty$;

2. *When* $\lambda^\sharp < \lambda < 1$, $S(\lambda) > U(\lambda)$, *and* Γ^s_λ *can be expressed as* $\{(u, v^s(u)) : b < u < \infty\}$ *with* $\lim_{u\to\infty} v^s(u) = 0$. *If* $u_0 \le b$ *or* $u_0 > b$ *and* $v_0 > v^u(u_0)$, *then* $(u(t), v(t)) \to (0, 0)$ *as* $t \to \infty$; *if* $u_0 > b$ *and* $0 < v_0 < v^s(u_0)$, *then either* $(u(t), v(t)) \to (\lambda, v_\lambda)$ *or a periodic orbit as* $t \to \infty$.

Proof We prove the case of $b < \lambda < \lambda^\sharp$, and the other case is similar. $S(\lambda) < U(\lambda)$ is from Propositions 2.2 and 2.3. From the proof of Propositions 2.2, the portion of Γ^u_λ from $(1, 0)$ to $(\lambda, U(\lambda))$ and the portion of Γ^u_λ from $(\lambda, U(\lambda))$ to $(b, 0)$ are both above the nullcline $v = f(u)$, then both portions are monotone curves. In particular the portion of Γ^u_λ from $(1, 0)$ to $(\lambda, U(\lambda))$ can be expressed as $\{(u, v^u(u)) : \lambda \le u < 1\}$. Now the portion of Γ^u_λ on the left of $(\lambda, U(\lambda))$ must be above the portion of Γ^u_λ from $(\lambda, U(\lambda))$ to $(b, 0)$, thus it is also above the nullcline $v = f(u)$. Hence as an invariant solution curve, Γ^u_λ can be parameterized by u for $b < u < 1$. Also since $S(\lambda) < U(\lambda)$, then the invariant solution curve on Γ^u_λ cannot tend to $(b, 0)$, then Γ^u_λ must extend to $u < b$ thus the solution curve on Γ^u_λ can be extended to $(0, 0)$. The remaining statements follow easily from comparison argument and Poincaré–Bendixson Theorem. □

Proposition 2.4 shows that, to completely determine the global dynamics of (1.2), one has to have more information on the existence, nonexistence, uniqueness and bifurcation of periodic orbits, which we will discuss in the next two sections. Here we show nonexistence of periodic orbits when λ is near b or 1.

Proposition 2.5 *For* $\lambda > b$ *but near* b, (1.2) *has no periodic orbit, and* Γ^s_λ *is a heteroclinic orbit connecting* $B = (b, 0)$ *and* $C = (\lambda, v_\lambda)$. *Similarly for* $\lambda < 1$ *but near* 1, (1.2) *has no periodic orbit, and* Γ^u_λ *is a heteroclinic orbit connecting* $A = (1, 0)$ *to* C.

Proof We recall from Proposition 2.2, $S(\lambda) \ge f(\lambda)$ for $\lambda \in (b, 1)$. For $\lambda > b$ and near b, if $S(\lambda) = f(\lambda)$, then Γ^s_λ is a heteroclinic orbit connecting B and C, and it is impossible to have a periodic orbit which is around C.

So we consider the case of $S(\lambda) > f(\lambda)$. Let R_1 be the region with vertices B, $Q_1 = (\lambda, S(\lambda))$, $Q_2 = (u_1, f(u_1))$, where $u_1 > \lambda$ satisfies $S(\lambda) = f(u_1)$, and $Q_3 = (u_1, 0)$. Between B and Q_1, the boundary of R_1 is Γ^s_λ, and all other parts of the boundary of R_1 are the line segments between Q_1, Q_2 and Q_3, and back to B. Notice that Q_2 is well-defined when λ is close to b since $S(\lambda) < f(\lambda)$.

Examining the vector field defined in (1.2), one can easily see that R_1 is negatively invariant. Since C is the unique equilibrium point in the positive quadrant, any periodic orbit must encircle it and must lie wholly in R_1. The divergence of the vector field (1.2) is

$$TrJ = g'(u)f(u) - g'(u)v + g(u)f'(u) + g(u) - g(\lambda),$$

and the value of TrJ in R_1 converges uniformly to $TrJ(B)$ when $\lambda \to b^+$. But $TrJ(B)$ is $g(b)f'(b) + g(b) - g(\lambda)$, which is positive for λ near b from (a1). Hence $TrJ(u, v) > 0$ for any $(u, v) \in R_1$. Then there is no periodic orbit in R_1 from Bendixson–Dulac's Criterion (see Hsu (2006) Theorem 6.1.2). From the Poincaré–Bendixson

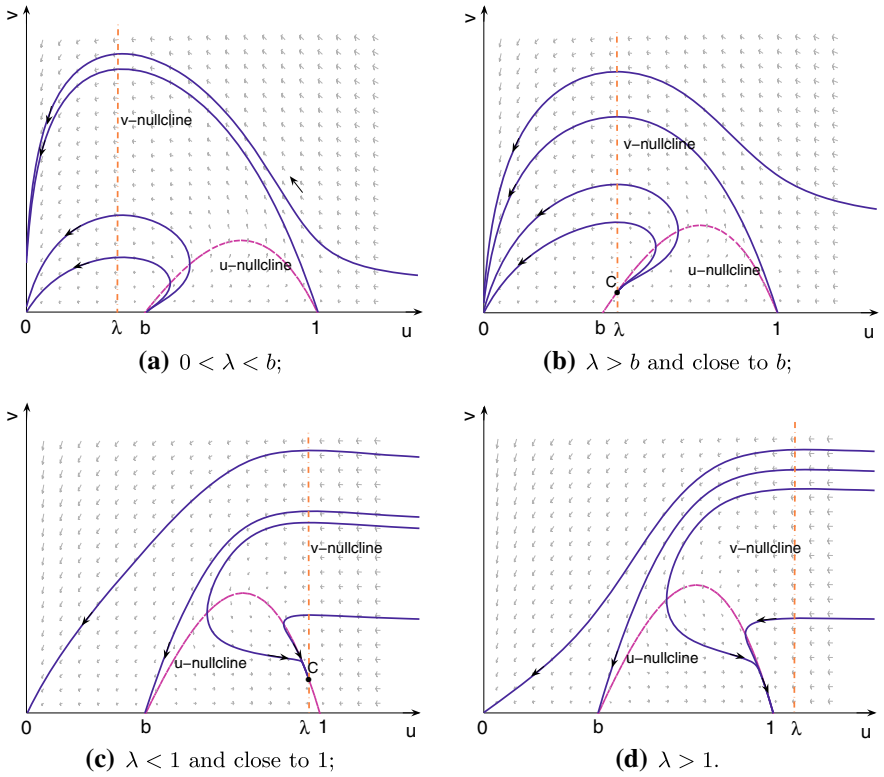

Fig. 2 Phase portraits of (1.2) with $f(u) = (a+u)(1-u)(u-b)/(bm)$ and $g(u) = mu/(a+u)$ where $a, m > 0$ and $0 < b < 1$. The *horizontal axis* is the prey population u, and the *vertical axis* is the predator population v. The *dashed curve* is the u-nullcline $v = f(u)$, and the *dashed-dotted vertical line* is the v-nullcline $g(u) = d$ or $u = \lambda$. Parameters used are given in Sect. 5.1 and Table 1

Theorem and the negative invariance of R_1, C is the α-limit set of Γ^s_λ. The result about λ near 1 can be proved similarly. □

To end this section we summarize discussions in this section to give a complete description of the dynamics for λ in some ranges:

Theorem 2.6 *Assume that f, g satisfy* (a1)–(a2). *Let $(u(t), v(t))$ be the unique solution of* (1.2) *with initial value (u_0, v_0) $(u_0, v_0 > 0)$. We follow the notations in Proposition* 2.4.

1. *For $0 < \lambda \le b$, then $(0,0)$ is globally asymptotically stable* (*see Fig.* 2a);
2. *For $\lambda > b$ but near b, if $u_0 \ge 1$ or $0 < u_0 < 1$ and $v_0 \ge v^u(u_0)$, then $(u(t), v(t)) \to (0,0)$ as $t \to \infty$; if $0 < u_0 < 1$ and $0 < v_0 < v^u(u_0)$, then $(u(t), v(t)) \to (0,0)$ as $t \to \infty$, hence $(0,0)$ is globally asymptotically stable* (*see Fig.* 2b);
3. *For $\lambda < 1$ but near 1, if $u_0 \le b$ or $u_0 > b$ and $v_0 > v^u(u_0)$, then $(u(t), v(t)) \to (0,0)$ as $t \to \infty$; if $u_0 > b$ and $0 < v_0 < v^s(u_0)$, then $(u(t), v(t)) \to (\lambda, v_\lambda)$ as $t \to \infty$* (*see Fig.* 2c);

4. *For* $\lambda \geq 1$, *if* $u_0 \leq b$ *or* $u_0 > b$ *and* $v_0 > v^u(u_0)$, *then* $(u(t), v(t)) \to (0, 0)$ *as* $t \to \infty$; *if* $u_0 > b$ *and* $0 < v_0 < v^s(u_0)$, *then* $(u(t), v(t)) \to (1, 0)$ *as* $t \to \infty$ (*see Fig.* 2d).

Proof For part 1 or part 4, there is no interior equilibrium point, thus there is no periodic orbit in the positive quadrant. From the observation of phase portraits, there is no loop of heteroclinic orbits in either case. So every orbit converges to a boundary equilibrium. Then the conclusions follow from similar arguments in the proof of Proposition 2.4. The results for part 2 or part 3 clearly follow from Propositions 2.4 and 2.5. □

In this section, we rigorously establish the existence of the heteroclinic loop for a unique $\lambda = \lambda^\sharp$. For the Lotka–Volterra case, this was proved in Conway and Smoller (1986) and was also observed in Bazykin (1998). As pointed out in Bazykin (1998), the critical parameter $\lambda^\sharp$ is a threshold between the oscillatory dynamics and the extinction dynamics. This will also be confirmed rigorously in Sects. 4 and 5.

3 Hopf bifurcation

In this section, we analyze the Hopf bifurcation occurring at $(\bar{\lambda}, v_{\bar{\lambda}})$ when taking λ as the bifurcation parameter. In addition to (a1)–(a2), we assume that

(a3) $f(u)$ and $g(u)$ are C^3 near $\lambda = \bar{\lambda}$ and $f''(\bar{\lambda}) < 0$.

Recall from Sect. 2 that the Jacobian matrix of the system (1.2) at (λ, v_λ) is

$$J = \begin{pmatrix} A(\lambda) & B(\lambda) \\ C(\lambda) & 0 \end{pmatrix},$$

where

$$A(\lambda) = g(\lambda) f'(\lambda), \quad B(\lambda) = -g(\lambda), \quad C(\lambda) = f(\lambda) g'(\lambda).$$

The characteristic equation is given by $\mu^2 - \mu T + D = 0$, where

$$T := tr\, J = A(\lambda); \qquad D := det\, J = -B(\lambda) C(\lambda).$$

From (a1), when $b < \lambda < \bar{\lambda}$, $T > 0$ and $D > 0$, so (λ, v_λ) is locally unstable; when $\bar{\lambda} < \lambda < 1$, $T < 0$ and $D > 0$, (λ, v_λ) is locally stable; $T(\bar{\lambda}) = 0$ and the Jacobian matrix $J(\bar{\lambda})$ has a pair of imaginary eigenvalues $\mu = \pm i\sqrt{-B(\bar{\lambda})C(\bar{\lambda})}$. Let $\mu = \beta(\lambda) \pm i\omega(\lambda)$ be the roots of $\mu^2 - \mu T + D = 0$ when λ is near $\bar{\lambda}$, then

$$\beta(\lambda) = \frac{A(\lambda)}{2}, \quad \omega(\lambda) = \frac{1}{2}\sqrt{-4B(\lambda)C(\lambda) - A(\lambda)^2}, \tag{3.1}$$

and

$$\beta'(\lambda) = \frac{1}{2}[g(\lambda) f'(\lambda)]' = \frac{1}{2}[g'(\lambda) f'(\lambda) + g(\lambda) f''(\lambda)]. \tag{3.2}$$

Thus from (a3),

$$\beta'(\lambda)\Big|_{\lambda=\bar{\lambda}} = \frac{1}{2}g(\bar{\lambda})f''(\bar{\lambda}) < 0,$$

From the Poincaré–Andronov–Hopf Bifurcation Theorem (for example, Theorem 3.1.3 in Wiggins (1990)), we know that the system (1.2) undergoes a Hopf bifurcation at $(\bar{\lambda}, v_{\bar{\lambda}})$ when $\lambda = \bar{\lambda}$. By further analysis of the normal form near the equilibrium (see Appendix), the direction of the Hopf bifurcation and the stability of bifurcating periodic orbits are determined by the first Lyapunov coefficient

$$a(\bar{\lambda}) = \frac{f'''(\bar{\lambda})g(\bar{\lambda})g'(\bar{\lambda}) + 2f''(\bar{\lambda})[g'(\bar{\lambda})]^2 - f''(\bar{\lambda})g(\bar{\lambda})g''(\bar{\lambda})}{16g'(\bar{\lambda})}. \tag{3.3}$$

The computation of $a(\bar{\lambda})$ is technical and we give the details in the Appendix. The derivation of the first Lyapunov coefficient follows a standard way. Our formula here follows Wiggins (1990), and other derivations like the ones in Hassard et al. (1981), Kuznetsov (2004) are similar but may differ by a positive constant multiple.

Now from Poincaré–Andronov–Hopf Bifurcation Theorem, we have:

Theorem 3.1 *Assume that f, g satisfy* (a1)–(a3). *Then the system* (1.2) *undergoes a Hopf bifurcation at $(\bar{\lambda}, v_{\bar{\lambda}})$; the Hopf bifurcation is supercritical and backward (respectively, subcritical and forward) if $a(\bar{\lambda}) < 0$ ($a(\bar{\lambda}) > 0$), where $a(\bar{\lambda})$ is defined in* (3.3). *In particular, the bifurcation is supercritical and backward if f and g also satisfy*

(a4) $f'''(\bar{\lambda}) \le 0$, *and* $g''(\bar{\lambda}) \le 0$.

Note that here we say a Hopf bifurcation with respect to parameter λ at $\lambda = \bar{\lambda}$ is backward (respectively, forward) if there is a small amplitude periodic orbit for each $\lambda \in (\bar{\lambda} - \varepsilon, \bar{\lambda})$ (respectively, $\lambda \in (\bar{\lambda}, \bar{\lambda} + \varepsilon)$) where $\varepsilon > 0$ is a small constant; and we say a Hopf bifurcation is supercritical (respectively, subcritical) if the bifurcating periodic solutions are orbitally asymptotically stable (respectively, unstable) (Kuznetsov 2004; Wiggins 1990). We apply Theorem 3.1 to several special cases of functional response $g(u)$.

1. Conway and Smoller (1986) considered the linear functional response $g(u) = u$. We notice that in this case, (3.3) is reduced to

$$a(\bar{\lambda}) = \frac{\bar{\lambda}f'''(\bar{\lambda}) + 2f''(\bar{\lambda})}{16} = \frac{\bar{\lambda}f''(\bar{\lambda})}{16}\left(\frac{f'''(\bar{\lambda})}{f''(\bar{\lambda})} + \frac{2}{\bar{\lambda}}\right), \tag{3.4}$$

   hence the Hopf bifurcation is supercritical and backward when $f'''(\bar{\lambda}) < 0$, which agrees with the result in Proposition 6 and equation (7) in Conway and Smoller (1986).
2. For Holling type II functional response $g(u) = u/(a + u)$, (3.3) is reduced to

$$a(\bar{\lambda}) = \frac{\bar{\lambda}f''(\bar{\lambda})}{16(a + \bar{\lambda})}\left(\frac{f'''(\bar{\lambda})}{f''(\bar{\lambda})} + \frac{2}{\bar{\lambda}}\right), \tag{3.5}$$

thus again the Hopf bifurcation is supercritical and backward when $f'''(\bar{\lambda}) \leq 0$. This also follows from (a4), as the type II response is concave.

3. For Holling type III functional response $g(u) = u^p/(a^p + u^p)$ (recall that $p > 1$), (3.3) is reduced to

$$a(\bar{\lambda}) = \frac{\bar{\lambda}^p f''(\bar{\lambda})}{16(a^p + \bar{\lambda}^p)} \left(\frac{f'''(\bar{\lambda})}{f''(\bar{\lambda})} + \frac{p+1}{\bar{\lambda}} \right), \tag{3.6}$$

thus the Hopf bifurcation is also supercritical and backward when $f''(\bar{\lambda}) < 0$ and $f'''(\bar{\lambda}) \leq 0$, even though $g(u)$ is not concave.

We notice that the Hopf bifurcation point $\lambda = \bar{\lambda}$ is at where the predator nullcline $u = \lambda$ intersects the prey nullcline $v = f(u)$ on the "top of the hump", the unique local maximum point of $v = f(u)$ in $(b, 1)$. Hence the condition $f''(\bar{\lambda}) < 0$ in (a3) is natural since $\bar{\lambda}$ is a local maximum. The requirement of C^3 smoothness in (a3) and the sign conditions of $f'''(\bar{\lambda})$ and $g''(\bar{\lambda})$ in (a4) are needed for the calculation of the first Lyapunov coefficient. As shown in examples above, these conditions are usually not restrictive in applications. On the other hand, (a3) only is sufficient to produce a Hopf bifurcation, while (a4) guarantees a supercritical Hopf bifurcation. Without (a4), a subcritical Hopf bifurcation is possible for (1.2), see Sects. 5.3–5.4 for examples.

The fact that the Hopf bifurcation is at the "top of the hump" is not particular for the system with strong Allee effect. For systems with logistic or weak Allee effect growth rate on the prey, the coexistence equilibrium is also stable when the vertical predator nullcline intersects with the "falling part" ($f'(u) < 0$) of the prey nullcline; and it is unstable if the intersection is on the "rising part" ($f'(u) > 0$) of the prey nullcline (see Hsu 1978; Rosenzweig 1969; Rosenzweig and MacArthur 1963). Hence the Hopf bifurcation occurs when the stability changes at the top of the hump.

We need to be cautious here and later that when $g(u)$ is not Lotka–Volterra type (linear), then $f(u)$ is not the growth rate per capita. For example for the type II response $g(u)$ and cubic $f(u)$, the system is in a form of

$$u' = \frac{mu}{a+u}\left[\frac{(1-u)(u-b)}{mb} - v\right], \quad v' = v\left(\frac{mu}{a+u} - d\right). \tag{3.7}$$

Hence the growth rate per capita in this system is $f(u)g(u)/u = b^{-1}(1-u)(u-b)/(a+u)$. For nonlinear functional responses, the biological meaning of $f(u)$ is not straightforward in our model: $f(u)g(u)$ is the growth rate while $g(u)$ is the functional response. $f(u)$ can be thought as a growth rate per capita factored by the functional response, and when $g(u)$ is linear then $f(u)$ is the growth rate per capita up to a multiplicative constant. In that sense, the Hopf bifurcation point is at the maximum value of this factored growth rate per capita. The non-monotonicity of $f(u)$ is an essential character of the Allee effect.

4 The uniqueness of limit cycle

The uniqueness and multiplicity of the limit cycles of planar systems is an important mathematical question related to the Hilbert 16th problem, and it is also practically useful in explaining the mechanical and natural oscillatory phenomena. The importance of limit cycles in predator–prey systems has been recognized by ecologists since the observation of Rosenzweig (1971) and May (1972), and the work of Albrecht et al. (1973, 1974) showed that the question is mathematically non-trivial but rather delicate. Since then many work on the existence (nonexistence) and uniqueness of limit cycles are carried out in, for example (Cheng 1981; Kuang and Freedman 1988; Xiao and Zhang 2003, 2008; Zeng et al. 1994; Zhang 1986). One of the main ideas is to translate a planar system into a Liénard system, which we also follow here. Let

$$\tau = \int_0^t g(u(t))dt, \qquad u = \lambda - x, \qquad v = v_\lambda e^y, \tag{4.1}$$

then (1.2) becomes a Liénard system

$$\begin{cases} \frac{dx}{d\tau} = v_\lambda e^y - f(\lambda - x), \\ \frac{dy}{d\tau} = 1 - \frac{d}{g(\lambda - x)}. \end{cases} \tag{4.2}$$

We recall some general existence/nonexistence and uniqueness of limit cycle results about the Liénard system (we follow the formulation in Xiao and Zhang (2003)): consider

$$\begin{cases} \frac{dx}{d\tau} = \phi(y) - F(x), \\ \frac{dy}{d\tau} = -h(x), \end{cases} \tag{4.3}$$

where $h(x)$ is continuous on an open interval (a_1, b_1), the functions $F(x)$ and $\phi(y)$ are continuously differentiable on open intervals (a_1, b_1) and (a_2, b_2), respectively. Here $-\infty \le a_i < 0 < b_i \le \infty$, $i = 1, 2$. Assume that the functions in (4.3) satisfy the following hypotheses:

(H1) $h(0) = 0$ and $xh(x) > 0$ for $x \neq 0$;
(H2) $\phi(0) = 0$ and $\phi'(y) > 0$ for $a_2 < y < b_2$;
(H3) the curve $\phi(y) = F(x)$ is well defined on all $x \in (a_1, b_1)$.

We also define $H(x) = \int_0^x h(y)dy$, and $F'(x) = r(x)$. Then the following result is due to Zhang (1986) (see Theorem 2.1 of Xiao and Zhang (2003)).

Theorem 4.1 *Suppose* (H1)–(H3) *are satisfied, the function* $r(x)/h(x)$ *is nondecreasing on* $(a_1, 0) \cup (0, b_1)$ *and is not constant in any small neighborhood of* $x = 0$. *Then* (4.3) *has at most one periodic orbit in the region* $\{(x, y) : a_1 < x < b_1\}$ *and it is stable if it exists.*

On the other hand, the following theorem is given in Zeng et al. (1994) (see Theorem 2.5 in Xiao and Zhang (2003)) and it is a simple way to determine the nonexistence of periodic orbits for (4.3).

Theorem 4.2 *Suppose* (H1)–(H3) *are satisfied, and for any* (u, x) *satisfying* $H(x) = H(u)$ *with* $a_1 < u < 0$ *and* $0 < x < b_1$,

$$\frac{r(u)}{h(u)} \geq \frac{r(x)}{h(x)} \qquad \left(or\ \frac{r(u)}{h(u)} \leq \frac{r(x)}{h(x)}\right)$$

holds. Then (4.3) *has no periodic orbits.*

We apply the above general results to the special Liénard system (4.2) (and consequently the original system (1.2)). Note that for (1.2), we only need to consider the case of $b + \varepsilon < \lambda < 1 - \varepsilon$ from Theorem 2.6. For λ in this range, it is easy to see that any periodic orbit must be contained in the region

$$\Omega_1 = \{(u, v) : b < u < 1,\ 0 < v < \infty\}.$$

The transformation in (4.1) maps the region Ω_1 to

$$\Omega_2 = \{(x, y) : \lambda - 1 < x < \lambda - b,\ -\infty < y < \infty\},$$

and the Liénard system (4.2) is the type in (4.3) with

$$\phi(y) = v_\lambda(e^y - 1), \quad F(x) = f(\lambda - x) - f(\lambda), \quad \text{and} \quad h(x) = \frac{d}{g(\lambda - x)} - 1.$$

Then it is easy to check that $h(x)$ is continuous on (a_1, b_1), $F(x)$ and $\phi(y)$ are continuously differentiable on (a_1, b_1) and (a_2, b_2), respectively; the conditions (H1)–(H3) hold for $(a_1, b_1) = (\lambda - 1, \lambda - b)$ and $(a_2, b_2) = (-\infty, \infty)$; and the dynamics of the system (4.2) in Ω_2 is equivalent to that of (1.2) in Ω_1 (see Lemma 3.2 of Xiao and Zhang (2003)). Now Theorems 4.1 and 4.2 become

Theorem 4.3 *Suppose that* f, g *satisfy* (a1)–(a2)*, and we define*

$$h_1(u) = \frac{f'(u)g(u)}{g(u) - g(\lambda)}. \tag{4.4}$$

1. *If* $h_1(u)$ *is nonincreasing in* $(b, \lambda) \cup (\lambda, 1)$*, then there is at most one periodic orbit of* (1.2) *in the region* $\Omega_1 = \{(u, v) : b < u < 1,\ 0 < v < \infty\}$;
2. *If for any* u_1, u_2 *satisfying*

$$\int_{u_1}^{\lambda} \frac{g(\lambda) - g(s)}{g(s)} ds = \int_{\lambda}^{u_2} \frac{g(s) - g(\lambda)}{g(s)} ds$$

with $b < u_1 < \lambda$ *and* $\lambda < u_2 < 1$,

$$h_1(u_1) \geq h_1(u_2) \quad (or \ \ h_1(u_1) \leq h_1(u_2)) \tag{4.5}$$

holds, then (1.2) *has no periodic orbits in* Ω_1.

Now we are ready to state a complete classification of phase portraits of (1.2) when $\lambda \in (b, \bar{\lambda})$:

Theorem 4.4 *Suppose that* f, g *satisfies* (a1)–(a4)*, and*

(a5) $h_1(u) = \frac{f'(u)g(u)}{g(u)-g(\lambda)}$ *is nonincreasing in* $(b, \lambda) \cup (\lambda, 1)$ *for each* $\lambda \in (b, \bar{\lambda})$.

Then in addition to the results in Theorem 2.6*, we also have*

$$b < \lambda^\sharp < \bar{\lambda}. \tag{4.6}$$

Moreover let $(u(t), v(t))$ *be the solution of* (1.2) *with positive initial value* (u_0, v_0)*, then*

1. *For* $b < \lambda < \lambda^\sharp$, $(u(t), v(t)) \to (0, 0)$ *as* $t \to \infty$ *and* $(0, 0)$ *is globally asymptotically stable* (*see Fig.* 3a);
2. *For* $\lambda = \lambda^\sharp$, *there exists a loop of heteroclinic orbits connecting two equilibrium points* $B = (b, 0)$ *and* $A = (1, 0)$; *if* (u_0, v_0) *is in the interior of the loop, then* $(u(t), v(t))$ *converges to the heteroclinic loop as* $t \to \infty$, *and if* (u_0, v_0) *is outside of the loop, then* $(u(t), v(t)) \to (0, 0)$ *as* $t \to \infty$ (*see Fig.* 3b);
3. *For* $\lambda^\sharp < \lambda < \bar{\lambda}$, *there exists a unique limit cycle such that if* (u_0, v_0) *is below the stable manifold of B, then* $(u(t), v(t))$ *converges to the limit cycle as* $t \to \infty$, *and if* (u_0, v_0) *is above the stable manifold of B, then* $(u(t), v(t)) \to (0, 0)$ *as* $t \to \infty$ (*see Fig.* 3c, d).

Proof Here we apply the global bifurcation theorem for the periodic orbits, see for example Alexander and Yorke (1978) (Theorem A), see also Chow and Mallet-Paret (1978), Wu (1998). The global bifurcation theorem asserts that the small amplitude periodic orbits near the Hopf bifurcation point $\lambda = \bar{\lambda}$ belong to a connected subset S_0 of $S \bigcup \{(\bar{\lambda}, \bar{T}, (\bar{\lambda}, v_{\bar{\lambda}}))\}$, where $\bar{T} = 2\pi/\omega(\bar{\lambda})$ and $S = \{(\lambda, T, (u_0, v_0)) \in (b, 1) \times \mathbb{R}^+ \times (\mathbb{R}^+)^2 : \ (u(t), v(t))$ is periodic$\}$. The periodic solution here has a minimal positive period which excludes equilibrium ones. Here T denotes the minimal period of the orbit, thus S catalogues the parameter, minimal period and initial condition of all non-stationary periodic solutions of (1.2). Moreover S_0 is either not compact, or $\overline{S_0} \backslash S_0$ contains another equilibrium point $(\lambda, T, (u, v))$. In the latter case, Hopf bifurcation must occur at $(\lambda, T, (u, v))$ with limiting minimal period T. But from our prior analysis, $(\bar{\lambda}, (\bar{\lambda}, v_{\bar{\lambda}}))$ is the only possible Hopf bifurcation point for (1.2), hence the latter alternative is not possible. Therefore S_0 is unbounded.

From Proposition 2.5, there are no periodic orbits for λ near $\lambda = b$ or $\lambda = 1$, and from Lemma 2.1, all periodic orbits are uniformly bounded for all $\lambda \in (b, 1)$. Hence S_0 possesses of periodic orbits with arbitrarily large period T. Since f and g satisfy (a1)–(a4), then the Hopf bifurcation is supercritical. From the condition (a5) and the

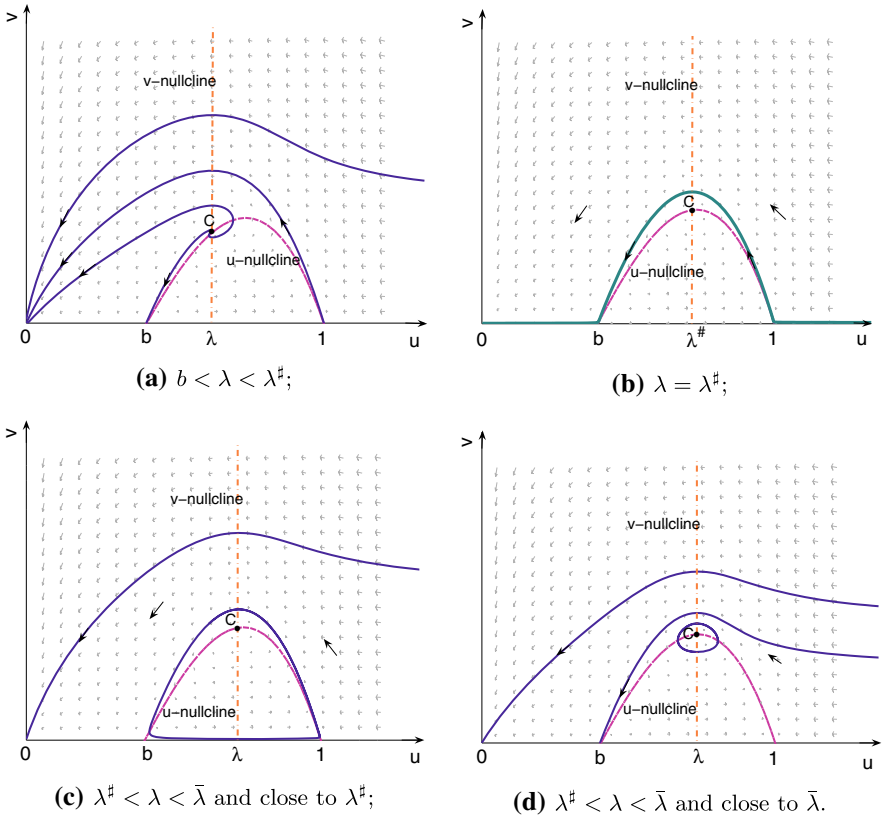

(a) $b < \lambda < \lambda^\sharp$; **(b)** $\lambda = \lambda^\sharp$;

(c) $\lambda^\sharp < \lambda < \bar{\lambda}$ and close to $\lambda^\sharp$; **(d)** $\lambda^\sharp < \lambda < \bar{\lambda}$ and close to $\bar{\lambda}$.

Fig. 3 Phase portraits of (1.2) with $f(u) = (a+u)(1-u)(u-b)/(bm)$ and $g(u) = mu/(a+u)$ where $a, m > 0$ and $0 < b < 1$ (continued). The *horizontal axis* is the prey population u, and the *vertical axis* is the predator population v. The *dashed curve* is the u-nullcline $v = f(u)$, and the *dashed-dotted vertical line* is the v-nullcline $g(u) = d$ or $u = \lambda$. Parameters used are given in Sect. 5.1 and Table 1

uniqueness proved in Theorem 4.3, the periodic orbit with $\lambda \in (b, \bar{\lambda})$ is stable and unique. Also there is no periodic orbits when $\lambda \in (b, b+\varepsilon)$. Hence there exists a $\lambda^* \in (b, \bar{\lambda})$ such that (1.2) has a unique limit cycle L_λ when $\lambda \in (\lambda^*, \bar{\lambda})$. All these limit cycles belong to S_0, and the period tends to infinity as $\lambda \to (\lambda^*)^+$.

Clearly the positive equilibrium (λ, v_λ) must be in the interior of L_λ. We fix a (u_*, v_*) near $(\lambda^*, v_{\lambda^*})$ which is in the interior of L_λ for all $\lambda \in (\lambda^*, \lambda^* + \varepsilon)$ with some small $\varepsilon > 0$. Let L_* be the ω-limit set of (u_*, v_*) when $\lambda = \lambda^*$. Then the Poincaré–Bendixson Theorem implies that L_* is one of the following three: an equilibrium point, a periodic orbit, or a loop of heteroclinic orbits.

We show that the first two alternatives are not possible. If L_* is a periodic orbit, then the stability of L_* implies the existence of a periodic orbit for each λ near λ^* with period near the one at L_*. But on the other hand there is a periodic orbit for $\lambda > \lambda^*$ such that the period tends to infinity as $\lambda \to (\lambda^*)^+$. That is a contradiction to the uniqueness of the limit cycle. If L_* is an equilibrium point, then L_* must be one of $(0, 0)$, $(b, 0)$ or $(1, 0)$. But

1. Since $(1, 0)$ is a saddle with the stable manifold being the u-axis, then L_* cannot be $(1, 0)$.
2. If L_* is $(0, 0)$, then from the continuous dependence of the solutions on the parameter λ, there exists a $T > 0$ such that $u(\lambda, T) < b/2$ for $\lambda \in (\lambda^* - \varepsilon, \lambda^* + \varepsilon)$, where $(u(\lambda, t), v(\lambda, t))$ is the solution with the parameter λ and initial value (u_*, v_*). But on the other hand, $u(\lambda, t) \geq b$ for $\lambda \in (\lambda^*, \lambda^* + \varepsilon)$ since it tends to a limit cycle whose u-value is less than b. That is a contradiction, thus L^* cannot be $(0, 0)$.
3. If L_* is $(b, 0)$, then the orbit starting from (u_*, v_*) is the stable manifold of $(b, 0)$. We can choose another (u_{**}, v_{**}) near (u_*, v_*) so that it is also in the interior of L_λ for all $\lambda \in (\lambda^*, \lambda^* + \varepsilon)$, and $v^{**}(T^{**}) > v^*(T^*)$ where $(u^i(t), v^i(t))$ is the solution of (1.2) with initial value (u_i, v_i), and T^i is the last time so that $u^i(T^i) = \lambda$, $i = *, **$. Then from Proposition 2.4, $(u^{**}(t), v^{**}(t)) \to (0, 0)$ as $t \to \infty$. Arguing the same way as the case of $L_* = (0, 0)$, we reach a contradiction with (u_{**}, v_{**}) is in the interior of L_λ for all $\lambda \in (\lambda^*, \lambda^* + \varepsilon)$. So $L_* = (b, 0)$ is also not possible.

Therefore L_* must be a loop of heteroclinic orbits, which can only occur at $\lambda = \lambda^\sharp$. Hence $\lambda^* = \lambda^\sharp$ which implies that $b < \lambda^\sharp < \bar{\lambda}$.

If there exists a limit cycle for some $\tilde{\lambda} \in (b, \lambda^\sharp)$, then the stability again shows the limit cycle exists for λ in an open interval, and the period tends to infinity when λ approaches the endpoints. Arguments above show that a loop of heteroclinic loop exists for the endpoint λ values. But that is not possible from the uniqueness of $\lambda^\sharp$ in Proposition 2.3. Hence for $\lambda \in (b, \lambda^\sharp)$, (1.2) has no limit cycle or heteroclinic loop, and the ω-limit set of any solution is a single boundary equilibrium point $(0, 0)$ since (λ, v_λ) is unstable. □

The assumption (a5) is mathematical rather than biological. But it can be easily verified for typical cases. Again we test our examples in previous section for the assumption (a5):

1. For $g(u) = u$,

$$h_1(u) = \frac{f'(u)u}{u - \lambda}, \quad \text{and} \quad h_1'(u) = \frac{f''(u)u^2 - \lambda[f'(u) + uf''(u)]}{(u - \lambda)^2}. \tag{4.7}$$

If $f(u) = b^{-1}(1 - u)(u - b)$ for which $\bar{\lambda} = (1 + b)/2$, then

$$h_1(u) = \frac{-2(u - \bar{\lambda})u}{b(u - \lambda)}, \quad \text{and} \quad h_1'(u) = \frac{-2[(u - \lambda)^2 + \lambda(\bar{\lambda} - \lambda)]}{b(u - \lambda)^2}. \tag{4.8}$$

Hence for any $\lambda < \bar{\lambda}$, $h_1'(u) \leq 0$ when $u \in (b, \lambda) \cup (\lambda, 1)$ hence (a5) and the results in Theorem 4.4 hold.

2. For Holling type II functional response $g(u) = mu/(a+u)$,

$$h_1(u) = \frac{(a+\lambda)uf'(u)}{a(u-\lambda)}, \quad \text{and}$$
$$h_1'(u) = \frac{(a+\lambda)[(u-\lambda)(uf''(u)+f'(u))-uf'(u)]}{a(u-\lambda)^2}. \tag{4.9}$$

Notice that the function $h_1(u)$ in (4.9) is only a rescaling of the one in (4.7), then (a5) also holds for $f(u) = b^{-1}(1-u)(u-b)$ and $g(u) = mu/(a+u)$, which is (3.7).

3. For Holling type III functional response $g(u) = u^p/(a^p+u^p)$,

$$h_1(u) = \frac{(a^p+\lambda^p)u^p f'(u)}{a^p(u^p-\lambda^p)}, \quad \text{and}$$
$$h_1'(u) = \frac{(a^p+\lambda^p)[f''(u)u^p(u^p-\lambda^p)-f'(u)pu^{p-1}\lambda^p]}{a^p(u^p-\lambda^p)^2}.$$

In the case of $f(u) = b^{-1}(1-u)(u-b)$,

$$h_1'(u) = \frac{-2(a^p+\lambda^p)[(u^p-(1+p)\lambda^p/2)^2+\lambda^p(p\bar{\lambda}u^{p-1}-(1+p)^2\lambda^p/4)]}{a^p b(u^p-\lambda^p)^2}$$
$$< \frac{-2(a^p+\lambda^p)[(u^p-(1+p)\lambda^p/2)^2+\lambda^p(p\bar{\lambda}b^{p-1}-(1+p)^2\lambda^p/4)]}{a^p b(u^p-\lambda^p)^2}.$$

Hence for any $p\bar{\lambda}b^{p-1} > (1+p)^2\lambda^p/4$, $h_1'(u) \le 0$ when $u \in (b,\lambda)\cup(\lambda,1)$.

In fact, for $g(u) = u$ or $g(u) = mu/(a+u)$, a more general condition on $f(u)$ can be derived for (a5). Define

$$G(\lambda,u) = (u-\lambda)[uf''(u)+f'(u)] - uf'(u), \tag{4.10}$$

where $(\lambda,u) \in [b,\bar{\lambda}]\times[b,1]$. Then (a5) holds if $G(\lambda,u) \le 0$ for all $(\lambda,u) \in [b,\bar{\lambda}]\times[b,1]$. It is easy to verify that $G(\lambda,\lambda) = -\lambda f'(\lambda) \le 0$ for all $\lambda \in [b,\bar{\lambda}]$. Also

$$\frac{\partial G}{\partial u}(\lambda,u) = (u-\lambda)[uf'''(u)+2f''(u)]. \tag{4.11}$$

Hence if $f(u)$ satisfies

(a6) $uf'''(u)+2f''(u) \le 0$ for all $u \in (b,1)$,

then $G_u \ge 0$ for $u \in (b,\lambda)$ and $G_u \le 0$ for $u \in (\lambda,1)$, hence $G(\lambda,u) \le 0$ for all $(\lambda,u) \in [b,\bar{\lambda}]\times[b,1]$. Therefore for the special cases of $g(u) = u$ and $g(u) = mu/(a+u)$, (a6) implies (a5).

Part 2 of Theorem 4.3 could lead to an estimate of the lower bound of $\lambda^\sharp$ if (a5) is satisfied:

Proposition 4.5 *Suppose that f, g satisfies (a1)–(a5), and λ_* is the unique root of the equation*

$$g(\lambda) = \frac{g(1)g(b)[f'(b) - f'(1)]}{f'(b)g(b) - f'(1)g(1)}. \tag{4.12}$$

Then for $b < \lambda < \lambda_*$, there is no periodic orbit for (1.2). In particular, $\lambda^\sharp \geq \lambda_*$.

Proof We apply the second part of Theorem 4.3. Since (a5) is satisfied, then $h_1(u_1) \leq h_1(u_2)$ for any $u_1 \in (b, \lambda)$ and $u_2 \in (\lambda, 1)$ if $h_1(b) \leq h_1(1)$, which is equivalent to

$$[f'(b)g(b) - f'(1)g(1)]g(\lambda) \leq g(1)g(b)[f'(b) - f'(1)], \quad \text{for } \lambda < \lambda_*. \tag{4.13}$$

Notice that from the definition of λ_*, we do have $g(b) < g(\lambda_*)$, and it follows that $b < \lambda_*$ from the monotonicity of $g(u)$. □

For $g(u) = u$ and $g(u) = mu/(a + u)$, (4.12) becomes

$$\lambda_* = \frac{b[f'(b) - f'(1)]}{bf'(b) - f'(1)}.$$

For $f(u) = b^{-1}(1 - u)(u - b)$, then $\lambda_* = 2b/(1 + b)$, and for $f(u) = (bm)^{-1}(1 - u)(u - b)(a + u)$,

$$\lambda_* = \frac{b(2a + b + 1)}{b^2 + ab + a + 1}.$$

5 Examples and discussion

In this section we apply our results to several examples which have been proposed in earlier investigations.

5.1 Cubic model with Holling II functional response

A prototypical model

$$\begin{cases} \frac{dU}{ds} = b_1 U(1 - U)\left(\frac{U}{b} - 1\right) - \frac{NUV}{1+AU}, \\ \frac{dV}{ds} = -d_2 V + \frac{NUV}{1+AU}, \end{cases} \tag{5.1}$$

was proposed by Owen and Lewis (2001), and also Petrovskii et al. (2002) (see also Morozov et al. 2004, 2006; Petrovskii et al. 2005). First we make a change of variables

$$t = b_1 s, \quad u = U, \quad v = V,$$

to obtain the dimensionless equation:

$$\begin{cases} \frac{du}{dt} = u(1-u)\left(\frac{u}{b}-1\right) - \frac{muv}{a+u}, \\ \frac{dv}{dt} = -dv + \frac{muv}{a+u}, \end{cases} \tag{5.2}$$

where $a = \frac{1}{A}$, $m = \frac{N}{Ab_1}$, $d = \frac{d_2}{b_1}$, and $0 < b < 1$. Let

$$f(u) = \frac{(a+u)(1-u)(u-b)}{bm}, \quad \text{and} \quad g(u) = \frac{mu}{a+u}. \tag{5.3}$$

Then (5.2) is in form of (1.2). Clearly $f(u)$ and $g(u)$ satisfy (a1) and (a2) if $0 < d < m$, which we always assume. Hence the results in Theorem 2.6 hold. The equilibrium points are

$$(0,0),\ (b,0),\ (1,0),\ (\lambda, v_\lambda) = \left(\lambda, \frac{(a+\lambda)(1-\lambda)(\lambda-b)}{mb}\right),$$

where $\lambda = \frac{ad}{m-d}$. The critical point $\bar{\lambda}$ of $f(u)$ in (b, λ) (which is also the Hopf bifurcation point) has the form:

$$\bar{\lambda} = \frac{b+1-a+\sqrt{(b+1-a)^2+3(ab+a-b)}}{3}$$

which is the larger root of $f'(\lambda) = 0$. At $\lambda = \bar{\lambda}$,

$$f''(\bar{\lambda}) = \frac{2(-3\bar{\lambda}+b+1-a)}{bm} < 0, \quad f'''(\bar{\lambda}) = \frac{-6}{bm} < 0, \quad g''(\bar{\lambda}) = \frac{-2ma}{(a+\bar{\lambda})^3} < 0.$$

Hence (a3) and (a4) are also satisfied. Thus the Hopf bifurcation at $\lambda = \bar{\lambda}$ is supercritical and backward and the bifurcating periodic solutions are orbitally asymptotically stable from Theorem 3.1.

Now we consider the uniqueness of limit cycle along the line of Theorem 4.4. We need to verify the condition (a5). In fact we can use the condition (a6) by calculating that

$$uf'''(u) + 2f''(u) = -\frac{18u + 4(a-1-b)}{bm}. \tag{5.4}$$

Hence $uf'''(u) + f''(u) \le 0$ for $u \in (b,1)$ if $7b + 2a - 2 \ge 0$, and the results in Theorem 4.4 hold if (a,b) satisfies $7b + 2a - 2 \ge 0$.

For the nonexistence of periodic orbits, we have a more specific result for (5.2):

Theorem 5.1 (5.2) *has no periodic orbits in the interior of the first quadrant if one of the following conditions is satisfied*:

1. $0 < a < 1, 0 < b < \frac{2(1-a)}{7}$ *and* $b < \lambda < \lambda_{**} = \frac{2(b+1-a)}{9}$; *or*
2. $\bar{\lambda} < \lambda < 1$.

Proof From the transformation in Sect. 4, (5.2) can be rewritten as the form of (4.2). And with f, g given in (5.3), it is in the form of (4.3) with

$$\phi(y) = v_\lambda(e^y - 1), \quad h(x) = \frac{(m-d)x}{m(\lambda - x)},$$
$$F(x) = \frac{x}{bm}[3\lambda^2 - 2(b+1-a)\lambda + b - (b+1)a + (b+1-a-3\lambda)x + x^2],$$

where $a_1 = \lambda - 1 < x < \lambda - b = b_1$ and $a_2 = -\infty < y < +\infty = b_2$. One can easily verify that the hypotheses (H1)–(H3) hold for this set of $\phi(y)$, $F(x)$ and $h(x)$.

We apply Theorem 4.2 directly. Then

$$r(u) = F'(u) = \frac{1}{bm}(3u^2 - 2(3\lambda - S_1)u + S_2 - 2S_1\lambda + 3\lambda^2),$$

where S_1, S_2 are defined by

$$S_1 = b + 1 - a, \quad S_2 = b - (b+1)a;$$

and also

$$H(u) = \int_0^u h(s)ds = \frac{ad}{m}\left(\ln\left|\frac{\lambda}{\lambda - u}\right| - \frac{u}{\lambda}\right).$$

If $H(u) = H(x)$ for $\lambda - 1 < u < 0$ and $0 < x < \lambda - b$, then

$$u - x + \lambda \ln\left|\frac{\lambda - u}{\lambda - x}\right| = 0,$$

which implies that $u + x < 0$ since $h(u)$ is convex on $(\lambda - 1, \lambda - b)$. From straightforward calculation, we obtain that for $\lambda - 1 < u < 0$ and $0 < x < \lambda - b$,

$$\frac{r(u)}{h(u)} - \frac{r(x)}{h(x)} = \frac{u - x}{b(m-d)ux}\left(ux[3(u+x) + 9\lambda - 2S_1] - (S_2 - 2S_1\lambda + 3\lambda^2)\lambda\right).$$

We notice that $S_2 - 2S_1\lambda + 3\lambda^2 = -mbf'(\lambda) < 0$ for $\lambda \in [b, \bar{\lambda})$ and $S_2 - 2S_1\lambda + 3\lambda^2 > 0$ for $\lambda \in (\bar{\lambda}, 1]$.

Now if $\lambda \in [b, \bar{\lambda})$ and $9\lambda + 2(a - 1 - b) = 9\lambda - 2S_1 \le 0$, then by using $u - x < 0$, $u + x < 0$, $ux < 0$, we obtain that

$$\frac{r(u)}{h(u)} - \frac{r(x)}{h(x)} > \frac{u - x}{b(m-d)}(9\lambda - 2S_1) \ge 0,$$

for all $\lambda - 1 < u < 0$ and $0 < x < \lambda - b$. Hence from Theorem 4.2, (5.2) has no periodic orbits in the first quadrant.

On the other hand, if $\bar{\lambda} < \lambda < 1$ and $\bar{\lambda} > \frac{5+2b-2a}{12}$, then by using similar arguments above, also $u + x < \lambda - 1$ and $S_2 - 2S_1\lambda + 3\lambda^2 > 0$, we have

$$\frac{r(u)}{h(u)} - \frac{r(x)}{h(x)} < \frac{u - x}{b(m - d)}(12\lambda + 2a - 2b - 5) < 0,$$

for all $\lambda - 1 < u < 0$ and $0 < x < \lambda - b$. It is easy to verify that for all $a, b > 0$, then $12\bar{\lambda} + 2a - 2b - 5 > 0$ holds. Hence again from Theorem 4.2, there is no periodic orbits in the first quadrant as long as $\bar{\lambda} < \lambda < 1$. □

Theorems 2.6 and 3.1, the second part of Theorems 5.1 and 4.4 (which holds when $7b + 2a \geq 2$) gives a complete rigorous global bifurcation diagram for the system (5.2) if (a, b) satisfies

$$a > 0, \quad 1 > b > 0, \quad \text{and} \quad 7b + 2a - 2 > 0. \tag{5.5}$$

That is, there exist two bifurcation points

$$\bar{\lambda} = \frac{b + 1 - a + \sqrt{(b + 1 - a)^2 + 3(ab + a - b)}}{3}, \quad \lambda^\sharp > \frac{b(2a + b + 1)}{b^2 + ab + a + 1};$$

with $b < \lambda^\sharp < \bar{\lambda} < 1$ such that

(i) When $0 < \lambda \leq b$, there is no periodic orbits and $(0, 0)$ is globally asymptotically stable from Theorem 2.6. (Fig. 2a)

(ii) When $b < \lambda < \lambda^\sharp$, there is no periodic orbits and $(0, 0)$ is globally asymptotically stable from Theorem 4.4. (Figs. 2b, 3a)

(iii) When $\lambda = \lambda^\sharp$, there is no periodic orbits and there is a loop of heteroclinic orbits from A to B then back to A (Theorem 4.4), and the loop separates the basins of attraction of $(0, 0)$ and the loop itself (attracting all initial values in the interior of the loop). (Fig. 3b)

(iv) When $\lambda^\sharp < \lambda < \bar{\lambda}$, there is a unique limit cycle, the stable manifold of $B = (b, 0)$ separates the basins of attraction of $(0, 0)$ and the limit cycle (Theorem 4.4); the limit cycle converges to the loop of heteroclinic orbits when $\lambda \to (\lambda^\sharp)^+$ (Theorem 4.4), and limit cycle emerges from the coexistence equilibrium (λ, v_λ) at $\lambda = \bar{\lambda}$ through a supercritical Hopf bifurcation (Theorem 3.1). (Fig. 3c, d)

(v) When $\bar{\lambda} < \lambda < 1$, there is no periodic orbits (Theorem 5.1), (λ, v_λ) is locally stable, and the basins of attraction of (λ, v_λ) and $(0, 0)$ are separated by the stable manifold of $(b, 0)$. (Fig. 2c)

(vi) When $\lambda \geq 1$, there is no periodic orbits, and the attractive basins of $(b, 0)$ and $(1, 0)$ are separated by the stable manifold Γ_λ^b of $(b, 0)$ (Theorem 2.6). (Fig. 2d)

We suspect that the parameter condition $7b + 2a - 2 > 0$ is only a technical condition which is needed for Theorem 4.4, and other theorems do not require this condition.

Table 1 Values of parameter m or λ in Figs. 2 and 3

Figure	Fig. 2a	Fig. 2b	Fig. 2c	Fig. 2d	Fig. 3a	Fig. 3b	Fig. 3c	Fig. 3d
m	2.5	2.1	1.52	1.45	1.8	1.6933	1.69	1.682
λ	0.3333	0.4545	0.9615	1.1111	0.625	0.7212	0.7246	0.7331

Recall that $\lambda = ad/(m-d)$

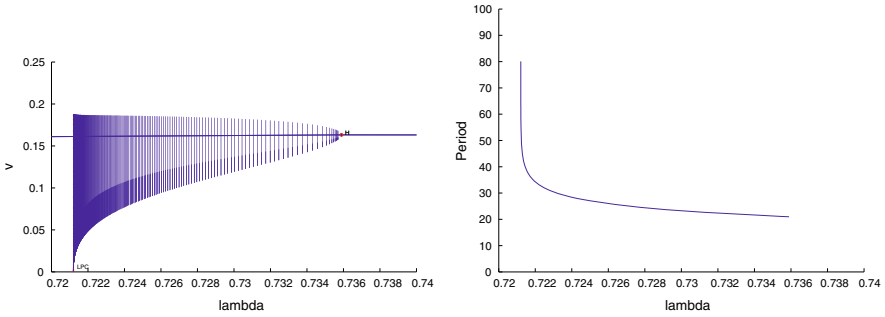

Fig. 4 Bifurcation diagrams of of the periodic orbits of (5.2) with $a = 0.5$, $b = 0.4$ and $d = 1$. The Hopf bifurcation point $\bar{\lambda}$ is 0.7359, and the heteroclinic point $\lambda^\sharp$ is 0.7212. The horizontal axis on the left and middle graphs is $\lambda \in [0.72, 0.74]$. *Left*: v-amplitude of the periodic orbits, where each *vertical line* represents the v-range of the limit cycle for that λ-value (the vertical axis is v); the almost *horizontal curve* in the center is the v value of the coexistence equilibrium; H is the Hopf bifurcation point $\lambda = \bar{\lambda}$, and LPG is the homoclinic point $\lambda = \lambda^\sharp$; *Right*: the period of the limit cycles (the vertical axis is the period T)

On the other hand, this condition holds if $1 > b > 2/7$ (the threshold is not too low) or $a > 1$.

The numerical phase portraits in Figs. 2 and 3 are generated using the Eq. (5.2) and they are produced by using `pplane7` package of `Matlab` developed by Polking and Arnold (2003). The parameters which we use are $a = 0.5$, $b = 0.4$ and $d = 1$, and different m-values (and corresponding λ-values) given in Table 1.

While Figs. 2 and 3 show the evolution of the phase portraits, the following Fig. 4 shows the bifurcation of the periodic orbits for (5.2) between $\lambda^\sharp < \lambda < \bar{\lambda}$. The bifurcation diagrams confirm the theoretical prediction of backward and supercritical Hopf bifurcation at $\lambda = \bar{\lambda}$. From the left panel of Fig. 4, one can see that the minimum of the predator population is nearly zero when λ is close to $\lambda^\sharp$, which increases the possibility of extinction. This is similar to the limit cycles in Rosenzweig–MacArthur model with logistic growth (Hsu and Shi 2009; Rosenzweig 1971) when $\lambda \to 0$ (λ is also the coordinate of the predator nullcline), which suggests that the paradox of enrichment destabilizes the population, and the oscillation of the population makes it more vulnerable to possible stochastic fluctuation. It is also clear from the right panel of Fig. 4 that the period of the limit cycle tends to ∞ as $\lambda \to (\lambda^\sharp)^+$, which is one of the alternatives in the global bifurcation theorem in Alexander and Yorke (1978), Chow and Mallet-Paret (1978), and Wiggins (1990). The bifurcation diagrams in Fig. 4 are generated by `MatCont` (Dhooge et al. 2003), which is a `Matlab` toolbox that for numerical bifurcation diagrams.

5.2 Cubic model with linear functional response

The same rigorous complete global bifurcation diagram for (5.2) also holds for the model with Lotka–Volterra interaction, which in dimensionless version is:

$$\begin{cases} \frac{du}{dt} = u(1-u)\left(\frac{u}{b}-1\right) - muv, \\ \frac{dv}{dt} = -dv + muv. \end{cases} \tag{5.6}$$

A global bifurcation analysis of (5.6) was given in Bazykin (1998) Section 3.5.5 and Conway and Smoller (1986), and a recent biological explanation of the bifurcation for (5.6) is given in van Voorn et al. (2007). Our results in this paper provide more rigorous verification of the rough picture in Conway and Smoller (1986), and the generalization to the system (1.2) shows that such global bifurcation hold for a much wider class of models. For (5.6),

$$f(u) = \frac{(1-u)(u-b)}{bm}, \quad \text{and} \quad g(u) = mu. \tag{5.7}$$

Our analysis in earlier sections shows for

$$f(u) = \frac{(1-u)(u-b)}{bm}, \quad \text{and} \quad g(u) = \frac{mu}{a+u}, \qquad a > 0, \tag{5.8}$$

(it corresponds to the system (3.7)), all calculations to verify the conditions (a1)–(a6) are similar to that of (5.1). One can easily verify that (a1)–(a4) and (a6) are satisfied for f, g in (5.7) and (5.8). Hence all results in Theorems 2.6, 3.1 and 4.4 hold. Moreover similar to Theorem 5.1, we can verify the nonexistence of periodic orbits discussed in previous subsection for $\lambda \in (\bar{\lambda}, 1)$:

1. For (5.6) (f, g in (5.7)),

$$\bar{\lambda} = \frac{1+b}{2}, \quad r(u) = \frac{2(\lambda-u)-(1+b)}{bm}, \quad h(u) = \frac{u}{\lambda-u}.$$

   After the same calculation in the proof of Theorem 5.1, we get

$$\frac{r(u)}{h(u)} - \frac{r(x)}{h(x)} = \frac{u-x}{bux}\left(2ux + [(1+b) - 2\lambda]\lambda\right) < 0$$

   for all $\lambda - 1 < u < 0$ and $0 < x < \lambda - b$. Hence there is no periodic orbits in the first quadrant, which provides a more precise result than that in Conway and Smoller (1986).
2. For (3.7) (f, g in (5.8)),

$$\bar{\lambda} = \frac{1+b}{2}, \quad r(u) = r(u) = \frac{2(\lambda-u)-(1+b)}{bm}, \quad h(u) = \frac{(m-d)u}{m(\lambda-u)},$$

and

$$\frac{r(u)}{h(u)} - \frac{r(x)}{h(x)} = \frac{m(u-x)}{b(m-d)ux}\,(2ux + [(1+b) - 2\lambda]\lambda) < 0$$

for all $\lambda - 1 < u < 0$ and $0 < x < \lambda - b$. Thus there is no periodic orbits.

Therefore the exact same global bifurcation scenario listed in Sect. 5.1 holds for (5.6) and (3.7) with

$$\bar{\lambda} = \frac{1+b}{2}, \quad \lambda^{\sharp} > \frac{2b}{1+b},$$

and here we only need (a, b) satisfies (compare to (5.5))

$$a > 0, \quad 1 > b > 0. \tag{5.9}$$

We also mention that an epidemic model with Allee effect was considered recently by Thieme et al. (2009):

$$\begin{cases} \frac{dS}{dt} = \sigma S(G(S)/\sigma - I), \\ \frac{dI}{dt} = I(\sigma S - \sigma S_*). \end{cases} \tag{5.10}$$

If we define $f(S) = G(S)/\sigma$ and $g(S) = \sigma S$, then (5.10) is in form of (1.2). The function $G(S)$ in Thieme et al. (2009) satisfies (a1), and $g(S)$ is linear. Hence if conditions on f in (a3), (a4) and (a6) are satisfied, then the results in this subsection hold for (5.10). We note that some results (but not all) which we proved in this paper were also proved in Thieme et al. (2009) for the special case (5.10), but our results hold for much more general cases. Similar epidemic models were also considered in Hilker et al. (2009). We thank an anonymous referee for bringing (Hilker et al. 2009; Thieme et al. 2009) to our attention.

5.3 Boukal–Sabelis–Berec model

Boukal et al. (2007) proposed a model which incorporates both the strong and weak Allee effect:

$$\begin{cases} \frac{dU}{ds} = AU\left(1 - \frac{U}{K}\right)\left(1 - \frac{B+C}{U+C}\right) - \frac{EU^n}{1+EHU^n}V, \\ \frac{dV}{ds} = -DV + \frac{EU^n}{1+EHU^n}V. \end{cases} \tag{5.11}$$

With change of variables:

$$u = \frac{U}{K}, \quad v = \frac{V}{K}, \quad t = As,$$

the system (5.11) is converted into

$$\begin{cases} \frac{du}{dt} = u(1-u)\left(1 - \frac{b+c}{u+c}\right) - \frac{eu^n}{1+ehu^n}v, \\ \frac{dv}{dt} = -dv + \frac{eu^n}{1+ehu^n}v, \end{cases} \tag{5.12}$$

where $b = B/K, c = C/K, e = EK^n/A, h = HA$ and $d = D/A$. When $0 < b < 1$, (5.12) exhibits a strong Allee effect in prey population densities and a type Holling II or III functional response of the predator, where b is the Allee threshold, and c is an auxiliary parameter ($c > 0$). In this subsection we only consider the case of $n = 1$ (type II or linear functional response).

First we consider the case of linear functional response $g(u) = eu$. Then (5.12) (with $h = 0$) becomes

$$\begin{cases} \frac{du}{dt} = u(1-u)\left(1 - \frac{b+c}{u+c}\right) - euv, \\ \frac{dv}{dt} = -dv + euv. \end{cases} \tag{5.13}$$

The conditions (a1)–(a3) can easily be verified. For condition (a6), we have

$$uf'''(u) + 2f''(u) = \frac{2(c+1)(c+b)(u-2c)}{e(u+c)^4}.$$

Hence if $c \geq 1/2$, then $uf'''(u) + 2f''(u) \leq 0$ for $u \leq 1$ so that (a6) holds for $u \in (b, 1)$, and the results in Theorems 2.6, 3.1 and 4.4 hold. Thus the global bifurcation for $\lambda \in (0, \bar{\lambda}) \bigcup (1, \infty)$ is similar to (5.2) if $c \geq 1/2$.

However the Allee effect growth function in (5.13) is more flexible than the ones in (5.2) or (5.6) (Boukal et al. 2007; Courchamp et al. 2008), and this shows on its dynamics. For parameters not in the range indicated above, (5.13) can have other richer dynamics. Indeed one can calculate that

$$\bar{\lambda} = \sqrt{c^2 + b + (b+1)c} - c,$$

thus if $b + (b+1)c > 8c^2$, then $\bar{\lambda} f'''(\bar{\lambda}) + 2f''(\bar{\lambda}) > 0$ and the Hopf bifurcation at $\lambda = \bar{\lambda}$ is *subcritical* and forward. This subcritical Hopf bifurcation only occurs for small c, and as we have seen that for large c, the dynamics of (5.13) is similar to (5.2) and (5.6).

With this subcritical Hopf bifurcation, for $\bar{\lambda} < \lambda < \bar{\lambda} + \epsilon$, the system possesses three locally stable states: the equilibrium points $(0, 0)$, (λ, v_λ) and a stable large amplitude periodic orbit which is close to the heteroclinic loop (see Fig. 5). And a small amplitude cycle is unstable, and it separates the basins of attraction of (λ, v_λ) and the large cycle. There is a largest $\tilde{\lambda} > \bar{\lambda}$ such that the system has periodic orbit for $\lambda \in (\lambda^\sharp, \tilde{\lambda}]$, and $\lambda = \tilde{\lambda}$ is a saddle-node bifurcation point for the periodic orbits. Near $\lambda = \tilde{\lambda}$, the two periodic orbits are nearly identical (see Fig. 5 Right). Note that unlike $\bar{\lambda}$ and $\lambda^\sharp$, $\tilde{\lambda}$ can only be determined numerically.

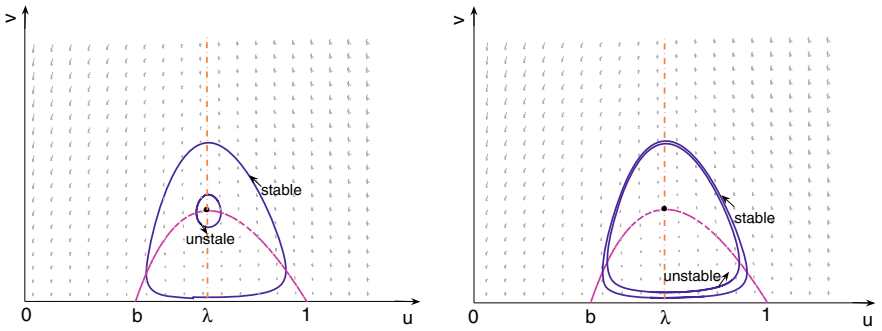

Fig. 5 Multiple periodic orbits in (5.13). Here $c = 0.3, b = 0.4, e = 1.\bar{\lambda} = 0.653939$ and Hopf bifurcation is subcritical. *Left*: $\lambda = 0.6540$, near subcritical Hopf bifurcation point; *Right*: $\lambda = 0.6544$, two nearly identical periodic orbits when λ is close to the saddle-node bifurcation point

For the case $h > 0$ (type II functional response), we let $a = 1/(eh)$, $m = 1/h$. Then (5.12) becomes

$$\begin{cases} \frac{du}{dt} = u(1-u)\left(1 - \frac{b+c}{u+c}\right) - \frac{muv}{a+u}, \\ \frac{dv}{dt} = -dv + \frac{muv}{a+u}, \end{cases} \tag{5.14}$$

which is in the form of (1.2) with

$$f(u) = \frac{1}{m}(1-u)(u-b)\left(\frac{u+a}{u+c}\right), \quad g(u) = \frac{mu}{a+u}.$$

The dynamics of (5.14) is similar to that of (5.13). In fact, one can calculate that

$$f''(u) = \frac{1}{m}\left(-2 + \frac{2M}{(u+c)^3}\right),$$
$$uf'''(u) + 2f''(u) = \frac{1}{m}\left(-4 + \frac{2(2c-u)M}{(u+c)^4}\right),$$

where

$$M = c^3 + (1-a+b)c^2 + (b-a-ba)c - ba.$$

One can see (a1), (a3) and (a6) are satisfied if c is sufficiently large, since

$$\lim_{c\to\infty} \frac{M}{(u+c)^3} = 1, \quad \lim_{c\to\infty} \frac{(2c-u)M}{(u+c)^4} = 2,$$

uniformly for $u \in [b, 1]$, and any $a > 0$, $1 > b > 0$. Hence the results in Theorems 2.6, 3.1 and 4.4 hold for (5.14) if c is large. On the other hand, subcritical Hopf bifurcation is still possible in this case for small c. We do not claim that we have a

complete classification of all possible dynamics of (5.14), but it certainly contains all dynamics of (5.13). Also we do not include a result on the nonexistence of periodic orbits for $\lambda \in (\bar{\lambda}, 1)$ since the calculation involved in applying Theorem 4.2 and 4.3 is too complicated here.

This example shows that a parameter other than the carrying capacity or the Allee threshold could have an influence on the dynamics by inducing a subcritical Hopf bifurcation. The parameter c in (5.12) affects the shape of the growth rate per capita, which we shall discuss more in Sect. 5.5 along with another example of subcritical Hopf bifurcation.

5.4 Another example of subcritical Hopf bifurcation

We have observed that in (5.13), the Hopf bifurcation may be supercritical or subcritical depending on a parameter value. Here we propose another model with that property:

$$\begin{cases} \frac{du}{dt} = u\left(1 + Be^{-\beta} - u - Be^{-\beta u}\right) - uv, \\ \frac{dv}{dt} = -dv + uv, \end{cases} \tag{5.15}$$

where $d > 0$, $B > 1$, and $B\beta > 1$. The functions $f(u) = 1 + Be^{-\beta} - u - Be^{-\beta u}$, $g(u) = u$ satisfy (a1)–(a3). The predator functional response is assumed to be Lotka–Volterra type to ease the computation, but we expect the results hold for more general functional responses. The growth rate per capita $f(u)$ is a logistic one subject to a loss term not due to the primary predator v. The carrying capacity is chosen as $1 + Be^{-\beta}$ so that $f(1) = 0$. The alternative predator is assumed to have a constant population, and the per capita predation rate $Be^{-\beta u}$ is a decreasing one. Hence in this model, the Allee effect is caused by another predator, which has been recognized as one of the possible causes of the Allee effect (see Berec et al. 2007; Gascoigne and Lipcius 2004, and Courchamp et al. (2008) Sections 2.3.2 and 3.2). Notice that the Allee effect is strong if $B > 1 + Be^{-\beta}$. This can also be viewed as a possible reduced two-predator and one prey model with different predator functional responses.

After direct computation, we have

$$f'(u) = -1 + B\beta e^{-\beta u} \quad \text{and} \quad f'(u) = 0 \text{ if and only if } u = \bar{\lambda} = \frac{1}{\beta} \ln B\beta;$$
$$f''(u) = -B\beta^2 e^{-\beta u} < 0; \quad f'''(u) = B\beta^3 e^{-\beta u} > 0 \text{ for all } u > 0.$$

In this case the expression of the first Lyapunov coefficient in (3.3) is reduced to

$$a(\bar{\lambda}) = \frac{\bar{\lambda} f'''(\bar{\lambda}) + 2f''(\bar{\lambda})}{16} = \frac{\bar{\lambda} f''(\bar{\lambda})}{16}\left(\frac{f'''(\bar{\lambda})}{f''(\bar{\lambda})} + \frac{2}{\bar{\lambda}}\right) = \frac{f''(\bar{\lambda})}{16}(2 - \ln B\beta). \tag{5.16}$$

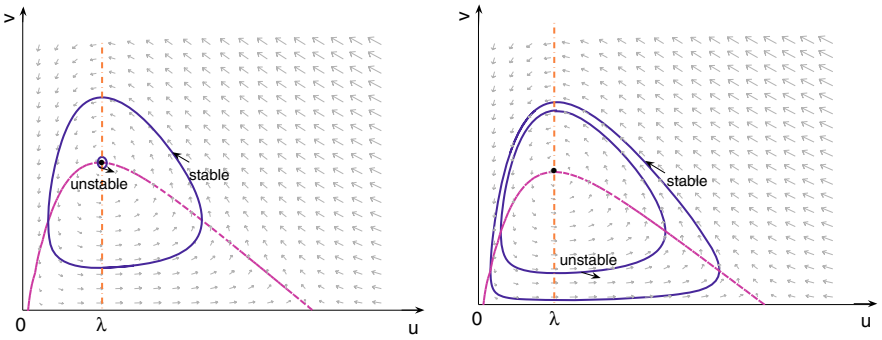

Fig. 6 Phase portraits of the system (5.15). Here $B = 1.2$, $\beta = 9$. *Left*: $d = 0.27140$, the Hopf bifurcation is subcritical and forward; *Right*: $d = 0.27309$, two nearly identical periodic orbits when d is close to the saddle-node bifurcation point

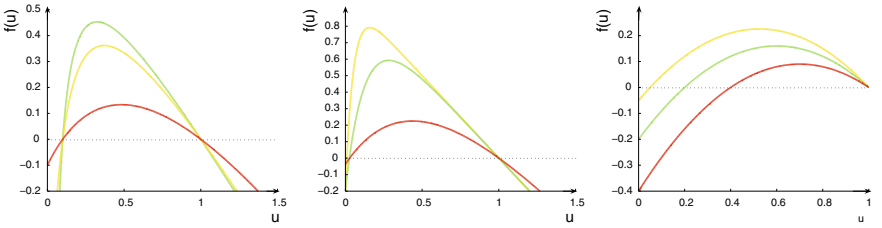

Fig. 7 Graphs of growth rate per capita functions with strong Allee effect. *Left*: $f(u) = e^{-1}(1-u)(u-b)/(u+c)$ with $b = 0.1, e = 1, c = 0.01, 0.1$ and 1 respectively from the higher to the lower ones; *Middle*: $f(u) = 1 + Be^{-\beta} - u - Be^{-\beta u}$ with $B = 1.2$, $\beta = 20, 8$ and 2 respectively from the higher to the lower ones; *Right*: $f(u) = (1-u)(u-b)$ with $b = 0.05, 0.2$ and 0.4 respectively from the higher to the lower ones. For all cases, the Hopf bifurcation point $\bar{\lambda}$ is the maximum point of $f(u)$

Then the Hopf bifurcation is supercritical and backward if $\ln B\beta < 2$, and it is subcritical and forward if $\ln B\beta > 2$. See Fig. 6 for phase portraits with two periodic orbits.

Note that the key of the subcritical Hopf bifurcation is that $f'''(u) > 0$. There is no obvious biological meaning of the third order derivative of the growth rate per capita function. But a comparison of the graphs of the growth rate per capita functions $f_1(u) = e^{-1}(1-u)(u-b)/(u+c)$ as in (5.13), $f_2(u) = 1 + Be^{-\beta} - u - Be^{-\beta u}$ as in (5.15) and $f_3(u) = (1-u)(u-b)$ as in (5.6) (see Fig. 7) reveals that if the "hump" is more or less symmetrical (f_3, or f_1 with large C or f_2 with small β), then the Hopf bifurcation is supercritical, but if the "hump" leans to $u = b$ (the survival threshold), then a subcritical Hopf bifurcation could occur.

5.5 General nonlinearities

Besides the examples given above, our main analytical results hold under very general conditions on $f(u)$ and $g(u)$. Here we discuss the restrictiveness of these conditions (a1)–(a6) and their applicability to predator–prey models with strong Allee effect

on the prey population. The condition (a1) and (a2) are our basic assumptions, and we always assume them. If (a1) is not satisfied, then $f(u)$ may have multiple positive "humps"; and in (a2), only monotonic functional responses are considered not the non-monotonic ones such as Holling type IV. In all known examples, (a3) ($f''(\bar{\lambda}) < 0$) is satisfied hence the Hopf bifurcation is non-degenerate. (a4) is a condition for supercritical Hopf bifurcation. In discussions in this section, we find that a supercritical bifurcation occurs for prototypical examples, but a subcritical bifurcation is also possible. (a5) is a more complicated condition to verify but restricted to the linear or type II functional responses, it becomes a simpler condition (a6). We note that if (a6) is satisfied, then the Hopf bifurcation must be supercritical as showed in (3.4) and (3.5).

In summary, while our results allow more generality on the nonlinear function, we state a result which is easier to verify the algebraic conditions, thus possibly more valuable to the applications:

Theorem 5.2 *Suppose that $f(u)$ satisfies (a1), (a3) and (a6), and $g(u)$ is one of the following*:

$$g(u) = u, \quad \text{or} \quad g(u) = \frac{mu}{a+u}, \quad a, m > 0. \tag{5.17}$$

Then by adapting a bifurcation parameter λ by defining

$$\lambda = d \ \text{ if } \ g(u) = u, \quad \text{or } \lambda = \frac{ad}{m-d} \ \text{ if } \ g(u) = \frac{mu}{a+u}, \tag{5.18}$$

there exist two bifurcation points $\lambda^\sharp$ and $\bar{\lambda}$ such that the dynamics of (1.2) can be classified as follows:

1. *If $0 < \lambda < \lambda^\sharp$, then the equilibrium $(0, 0)$ is globally asymptotically stable*;
2. *If $\lambda^\sharp < \lambda < \bar{\lambda}$, then there exists a unique limit cycle, and the system is globally bistable with respect to the limit cycle and $(0, 0)$*;
3. *If $\bar{\lambda} < \lambda < 1$, and if there is no periodic orbit, then the system is globally bistable with respect to the coexistence equilibrium (λ, v_λ) and $(0, 0)$*;
4. *If $\lambda > 1$, then the system is globally bistable with respect to $(1, 0)$ and $(0, 0)$.*

We note that the nonexistence of periodic orbits for $\bar{\lambda} < \lambda < 1$ can be proved using Theorem 4.2, which has been showed for some examples in Sects. 5.1, 5.2 and 5.4.

For the applicability of Theorem 5.2, we verify various typical growth rates with Allee effect for the conditions (a1), (a3) (a4), and (a6). Here we choose a collection of 6 growth rate per capita functions from Table 3.1 of Courchamp et al. (2008) (see also Table 1 of Boukal and Berec (2002)), and verify the range of parameters so that the conditions (a1), (a3), (a4) and (a6) are satisfied. We list the parameter restrictions when $g(u) = u$ in Table 2, and the one with $g(u) = u/(a+u)$ in Table 3. In Table 2, the restriction for (P1), (P2) and (P3) are all natural ones, hence Theorem 5.2 holds for all parameter ranges; for (P4), (P5) and (P6), some additional mathematical conditions are needed for Theorem 5.2, and different dynamics could exist for other parameter ranges. For Table 3, some restriction on the parameters are always needed for each example. Outside of the parameter ranges given in Tables 2 and 3, the system could have other dynamical behavior like multiple periodic orbits.

Table 2 Validity of conditions (a1), (a3), (a4) and (a6) when the functional response is linear $g(u) = u$

Per capita growth rate	Parameter constraints	(a1)	(a3)	(a4)	(a6)
(P1) Edelstein (1998)					
$r - b(u-e)^2$	$e^2 b > r$	$f(a \pm \sqrt{r/b}) = 0$ $\bar{\lambda} = e$	$f''(\bar{\lambda}) = -2b < 0$	$f'''(\bar{\lambda}) = 0$	$F(u) = -4b < 0$
(P2) Lewis and Kareiva (1993)					
$r(1-\frac{u}{K})(\frac{u}{K}-\frac{A}{K})$	$0 < A < K$	$f(A) = f(K) = 0$ $\bar{\lambda} = \frac{A+K}{2}$	$f''(\bar{\lambda}) = -\frac{2r}{K^2} < 0$	$f'''(\bar{\lambda}) = 0$	$F(u) = -\frac{4r}{K^2} < 0$
(P3) Gruntfest et al. (1997)					
$r(1-\frac{u}{K})(\frac{u}{A}-1)$	$0 < A < K$	$f(A) = f(K) = 0$ $\bar{\lambda} = \frac{A+K}{2}$	$f''(\bar{\lambda}) = -\frac{2r}{KA} < 0$	$f'''(\bar{\lambda}) = 0$	$F(u) = -\frac{4r}{KA} < 0$
(P4) Wilson and Bossert (1971)					
$(1-u)(1-\frac{b+c}{u+c})$	$0 < b < 1 \le 2c$ $M = (c+b)(c+1)$	$f(b) = f(1) = 0$ $\bar{\lambda} = -c + \sqrt{M}$	$f''(\bar{\lambda}) = \frac{-2M}{(\bar{\lambda}+c)^3} < 0$	$f'''(\bar{\lambda}) = \frac{6M}{(\bar{\lambda}+c)^4} > 0$	$F(u) = \frac{2M(u-2c)}{(u+c)^4} < 0$
(P5) Takeuchi (1996)					
$b + \frac{(e-u)u}{1+cu}$	$b < 0, \frac{e+bc+\sqrt{M}}{4} < \frac{1}{c}$ $M = (e+bc)^2 + 4b > 0$	$f\left(\frac{(e+bc)\pm\sqrt{M}}{2}\right) = 0$ $\bar{\lambda} = \frac{-1+\sqrt{1+ec}}{c}$	$f''(\bar{\lambda}) = \frac{-2(ce+1)}{(1+c\bar{\lambda})^3} < 0$	$f'''(\bar{\lambda}) = \frac{6c(ce+1)}{(1+c\bar{\lambda})^4} > 0$	$F(u) = \frac{2(1+ec)(cu-2)}{(1+cu)^4} < 0$
(P6) Jacobs (1984)					
$r_0 + \frac{ebu}{u+b} - cu$	$r_0 < 0, \frac{M+\sqrt{M^2+4r_0bc}}{4bc} < 1$ $M = r_0 + b(e-c) > 2\sqrt{-r_0bc}$	$f\left(\frac{M\pm\sqrt{M^2+4r_0bc}}{2c}\right) = 0$ $\bar{\lambda} = -b + \frac{b\sqrt{ec}}{c}$	$f''(\bar{\lambda}) = \frac{-2eb^2}{(\bar{\lambda}+b)^3} < 0$	$f'''(\bar{\lambda}) = \frac{6eb^2}{(\bar{\lambda}+b)^4} > 0$	$F(u) = \frac{2eb^2(u-2b)}{(u+b)^4} < 0$

In this case the function $f(u)$ is the same as the growth rate per capita. Here $F(u) = uf'''(u) + 2f''(u)$, and the code of the functions is the same as in Table 3.1 of Courchamp et al. (2008). The reference where the model first appeared is listed after the code. Parameters not specified in "Parameter constraints" are assumed to be positive

Table 3 Validity of conditions (a1) and (a6) when the functional response is Type II $g(u) = u/(a+u)$

Code	Parameter constraints	(a1)	(a3)	(a4)	(a6)
(P1)	$e^2 b > r$	$f(e \pm \sqrt{r/b}) = 0$	$f''(\bar{\lambda}) = -2\sqrt{M} < 0$	$f'''(\lambda) = -6b < 0$	$F(u) = 2b(-9u + 4e - 2a) < 0$
		$\bar{\lambda} = \dfrac{b(2e-a) + \sqrt{M}}{3b}$			
	$-5e + 9\sqrt{\dfrac{r}{b}} - 2a < 0$	$M = b^2(2e-b)^2$ $+3b(r + 2eba - be^2)$			
(P2)	$0 < A < K$	$f(A) = f(K) = 0$	$f''(\bar{\lambda}) = -\dfrac{2rM}{K^2} < 0$	$f'''(\lambda) = -\dfrac{6r}{K^2} < 0$	$F(u) = \dfrac{2r(-7A + 2K - 2a)}{K^2} < 0$
		$\bar{\lambda} = \dfrac{K + A - a + \sqrt{M}}{3}$			
	$-7A + 2K - 2a < 0$	$M = K^2 + A^2 + a^2$ $+(K+A)a - KA$			
(P3)	$0 < A < K$	$f(A) = f(K) = 0$	$f''(\bar{\lambda}) = -\dfrac{2rM}{KA} < 0$	$f'''(\lambda) = -\dfrac{6r}{KA} < 0$	$F(u) = \dfrac{2r(-7A + 2K - 2a)}{KA} < 0$
		$\bar{\lambda} = \dfrac{K + A - a + \sqrt{M}}{3}$			
	$-7A + 2K - 2a < 0$	$M = K^2 + A^2 + a^2$ $+(K+A)a - KA$			
(P4)	$0 < b < 1$	$f(b) = f(1) = 0$	$f''(\bar{\lambda}) = -2\left(1 + \dfrac{c-a}{(\bar{\lambda}+c)^3}\right) < 0$	$f'''(\lambda) = \dfrac{6M(c-a)}{(\bar{\lambda}+c)^4} > 0$	$F(u) = -4 + \dfrac{2M(u-2c)}{(u+c)^4} < 0$
		$\bar{\lambda}$ Satisfies $L_1(\bar{\lambda}) = 0$			
	c Large	$M = c^3 + (1-a+b)c^2$ $+(b-a-ba)c - ba$			
(P5)	$b < 0$	$f\left(\dfrac{M \pm \sqrt{M^2 + 4b}}{2}\right) = 0$	$f''(\bar{\lambda}) = -2\left(\dfrac{1}{c} + \dfrac{N}{(1+c\bar{\lambda})^3}\right) < 0$	$f'''(\lambda) = \dfrac{6cN}{(1+c\bar{\lambda})^4} > 0$	$F(u) = -\dfrac{4}{c} + \dfrac{2N(2-cu)}{(1+cu)^4} < 0$
	$M = e + bc > 2\sqrt{-b}$,	$\bar{\lambda}$ Satisfies $L_2(\bar{\lambda}) = 0$			
	c Large	$N = (1/c + e)(ac - 1) > 0$			

Table 3 continued

Code	Parameter constraints	(a1)	(a3)	(a4)	(a6)
(P6)	$r_0 < 0$, $\frac{M+\sqrt{M^2+4r_0bc}}{4bc} < 1$ $M = r_0 + b(e-c) > 2\sqrt{-r_0bc}$ $b \le a$	$f\left(\frac{M \pm \sqrt{M^2+4r_0bc}}{2c}\right) = 0$ $\bar{\lambda}$ Satisfies $L_3(\bar{\lambda}) = 0$ $N = b^2e(b-a)$	$f''(\bar{\lambda}) = -2\left(c + \frac{N}{(\bar{\lambda}+b)^3}\right) \ge 0$	$f'''(\lambda) = \frac{-6N}{(\bar{\lambda}+b)^4} > 0$	$F(u) = -4c + \frac{2N(2b-u)}{(u+b)^4} < 0$

In this case the function $f(u)g(u)/u = f(u)/(a+u)$ is the growth rate per capita. Here $F(u) = uf'''(u) + 2f''(u)$, and $f(u)$ are the same ones given in Table 2 with the corresponding codes. Parameters not specified in "Parameter Constraints" are assumed to be positive. The function L_i are defined as $L_1(\bar{\lambda}) = -2\bar{\lambda}^3 + (1+b-3c-a)\bar{\lambda}^2 + 2c(1+b-a)\bar{\lambda} + ca(1+b) - b(c-a) = 0$; $L_2(\bar{\lambda}) = -2c\bar{\lambda}^3 + ((e+bc)c - (3+ac))\bar{\lambda}^2 + 2(e+bc-a)u + ea + b = 0$; $L_3(\bar{\lambda}) = -2c\bar{\lambda}^3 + (r_0 + eb - ba - 4)\bar{\lambda}^2 + 2(r_0 + b(e-c) - a)b\bar{\lambda} + b^2(r_0 + (e-c)a) = 0$

6 Concluding remarks

Oscillatory behavior in predator–prey (consumer-resource) interaction has been an important topic in population dynamics since the pioneer work of Rosenzweig and MacArthur (1963), Rosenzweig (1971), and May (1972) etc. Global dynamical behavior such as global asymptotic stability of coexistence equilibrium, uniqueness and stability of limit cycle for predator–prey system with logistic type prey growth is now well-known (see Cheng 1981; Hsu 1978; Kuang and Freedman 1988; Xiao and Zhang 2003). In this article we rigourously establish the global bifurcation of a class of general predator–prey system with prey growth satisfying a strong Allee effect type growth pattern. The key bifurcation parameter λ is the location of the predator nullcline $u = \lambda$. While it is clear that when λ is below the prey extinction threshold b, the prey will become extinct, and consequently the predator will also starve to die, we show that there exists a higher threshold $\lambda^\sharp$ such that when $\lambda < \lambda^\sharp$, then the predator invasion leads to the extinction of both species, this phenomenon is called *overexploitation* Rosenzweig (1971). Mathematically it means the global stability of the equilibrium at $(0, 0)$, which is rigorously proved here. The threshold $\lambda^\sharp$ is at the unique point where a point-to-point heteroclinic orbit loop exists.

When λ moves across $\lambda = \lambda^\sharp$, a limit cycle appears as an alternative stable state, which can be established if initially the prey is over the self-growth threshold b, and the initial amount of the predator is under the overexploit threshold to make a successful invasion. This picture changes again when it moves past $\bar{\lambda}$, the alternative stable state of limit cycle switches to a coexistence equilibrium point, and the oscillation dies down to the stable equilibrium. Finally when λ is larger than 1, which is the carrying capacity of the prey population, the alternative stable state becomes the prey-only equilibrium, in which the predator species is not able to establish itself and will become extinct. For these cases, higher initial predator density will always lead to the overexploitation. Our rigorous analysis of the phase planes complements with several recent discussion of the ecological scenarios in Berec et al. (2007), Boukal et al. (2007), van Voorn et al. (2007), and Zhou et al. (2005).

Our rigorous analysis can be applied to most existing predator–prey models with strong Allee effect on the prey population, as shown in the examples in Sect. 5. The choices of the growth rate per capita (or "factored" growth rate per capita) $f(u)$ are listed in Tables 2 and 3, and our results are most complete when the functional response $g(u)$ is linear or Holling type II. This demonstrates the robustness of our results, and the results do not depend on the specific algebraic forms or parametrization of the nonlinear functions in the models.

On the other hand, besides the "basic" dynamics evolution shown above (or see Theorem 5.2), we also show that the predator–prey systems with Allee effect could have even richer dynamic structure like multiple limit cycles. Results from Liénard systems can be used to prove the uniqueness of limit cycle in certain cases, but the exact number of multiple cycles is not known yet analytically. The examples in Sects. 5.3 and 5.4 show the subtleness of the parameter choices in the Allee effect growth functions.

We do not consider the system with non-monotonic functional response, which has been recently considered in Aguirre Pablo et al. (2009) and González-Olivares et al. (2006). We do not include the spatial effect in this article. Some recent numerical

investigation of the reaction-diffusion models with strong Allee effect have shown complex dynamics (Morozov et al. 2004, 2006; Petrovskii et al. 2005, 2002), and our complete analysis of the ODE model will give new suggestions of numerical or analytical approach to the spatiotemporal models with Allee effect.

Acknowledgments We thank the anonymous referees for their helpful suggestions which greatly improve the earlier version of the manuscript.

7 Appendix

Here we give the calculation leading to the formula (3.3). First we translate the equilibrium (λ, v_λ) to the origin by the translation $\tilde{u} = u - \lambda$, $\tilde{v} = v - v_\lambda$. For the sake of convenience, we still denote $\tilde{u}$ and $\tilde{v}$ by u and v, respectively. Thus the system (1.2) becomes

$$\begin{cases} \frac{du}{dt} = g(u+\lambda)\left(f(u+\lambda) - (v+v_\lambda)\right), \\ \frac{dv}{dt} = (v+v_\lambda)\left(-d + g(u+\lambda)\right). \end{cases} \tag{7.1}$$

Rewrite the system (7.1) as follows:

$$\begin{cases} \frac{du}{dt} = g(u+\lambda)f(u+\lambda) - g(\lambda)f(\lambda) - [g(u+\lambda)(v+v_\lambda) - g(\lambda)v_\lambda], \\ \frac{dv}{dt} = -dv + [g(u+\lambda)(v+v_\lambda) - g(\lambda)v_\lambda]. \end{cases}$$

Computing the Taylor expansion of related functions:

$$\begin{aligned} &(v+v_\lambda)g(u+\lambda) - g(\lambda)v_\lambda \\ &\quad = a_{10}u + a_{01}v + a_{20}u^2 + a_{11}uv + a_{30}u^3 + a_{21}u^2v + O(|u|^4,\ |u|^3|v|), \end{aligned}$$

and

$$g(u+\lambda)f(u+\lambda) - g(\lambda)f(\lambda) = b_{10}u + b_{20}u^2 + b_{30}u^3 + O(|u|^4),$$

where

$$\begin{aligned} a_{10} &= g'(\lambda)v_\lambda, \quad a_{20} = \frac{1}{2}g''(\lambda)v_\lambda, \quad a_{30} = \frac{1}{6}g'''(\lambda)v_\lambda, \\ a_{01} &= g(\lambda), \qquad a_{11} = g'(\lambda), \qquad a_{21} = \frac{1}{2}g''(\lambda), \end{aligned}$$

and

$$b_{10} = (fg)'(\lambda), \quad b_{20} = \frac{1}{2}(fg)''(\lambda), \quad b_{30} = \frac{1}{6}(fg)'''(\lambda),$$

then the system (7.1) becomes

$$\begin{pmatrix} \frac{du}{dt} \\ \frac{dv}{dt} \end{pmatrix} = J \begin{pmatrix} u \\ v \end{pmatrix} + \begin{pmatrix} F_1(u, v, \lambda) \\ F_2(u, v, \lambda) \end{pmatrix}, \tag{7.2}$$

where

$$F_1(u, v, \lambda) = (b_{20} - a_{20})u^2 - a_{11}uv + (b_{30} - a_{30})u^3 - a_{21}u^2v + O(|u|^4, |u|^3|v|),$$
$$F_2(u, v, \lambda) = a_{20}u^2 + a_{11}uv + a_{30}u^3 + a_{21}u^2v + O(|u|^4, |u|^3|v|).$$

Define a matrix

$$P := \begin{pmatrix} 1 & 0 \\ N & M \end{pmatrix},$$

where $N = -\frac{A(\lambda)}{2B(\lambda)}$, and $M = -\frac{\sqrt{-4B(\lambda)C(\lambda)-A^2(\lambda)}}{2B(\lambda)}$. Then

$$P^{-1} = \begin{pmatrix} 1 & 0 \\ -\frac{N}{M} & \frac{1}{M} \end{pmatrix},$$

and when $\lambda = \bar{\lambda}$,

$$N_- := N\,|_{\lambda=\bar{\lambda}} = 0,$$
$$M_- := M\,|_{\lambda=\bar{\lambda}} = -\frac{\sqrt{-4B(\bar{\lambda})C(\bar{\lambda})}}{2B(\bar{\lambda})} = \sqrt{\frac{f(\bar{\lambda})g'(\bar{\lambda})}{g(\bar{\lambda})}}.$$

By using the linear transformation

$$\begin{pmatrix} u \\ v \end{pmatrix} = P \begin{pmatrix} x \\ y \end{pmatrix},$$

the system (7.2) becomes

$$\begin{pmatrix} \frac{dx}{dt} \\ \frac{dy}{dt} \end{pmatrix} = J(\lambda) \begin{pmatrix} x \\ y \end{pmatrix} + \begin{pmatrix} F^1(x, y, \lambda) \\ F^2(x, y, \lambda) \end{pmatrix}. \tag{7.3}$$

Here

$$J(\lambda) = \begin{pmatrix} \beta(\lambda) & -\omega(\lambda) \\ \omega(\lambda) & \beta(\lambda) \end{pmatrix},$$

where $\beta(\lambda)$ and $\omega(\lambda)$ are defined in (3.1), and

$$\begin{aligned} F^1(x,y,\lambda) &= F_1(x, Nx+My, \lambda) \\ &:= A_{20}x^2 + A_{11}xy + A_{21}x^2y + A_{30}x^3 + O(|x|^4) + O(|x|^4, |x|^3|y|), \\ F^2(x,y,\lambda) &= -\frac{N}{M}F_1(x, Nx+My, \lambda) + \frac{1}{M}F_2(x, Nx+My, \lambda) \\ &:= B_{20}x^2 + B_{11}xy + B_{30}x^3 + B_{21}x^2y + O(|x|^4, |x|^3|y|), \end{aligned}$$

where

$$\begin{aligned} A_{20} &= (b_{20} - a_{20}) - a_{11}N, \quad & A_{11} &= -a_{11}M, \\ A_{30} &= (b_{30} - a_{30}) - a_{21}N, \quad & A_{21} &= -a_{21}M, \\ B_{20} &= \frac{1}{M}(a_{20} + a_{11}N), & B_{11} &= a_{11}, \\ B_{30} &= \frac{1}{M}(a_{30} + a_{21}N), & B_{21} &= a_{21}. \end{aligned}$$

Rewrite the system (7.3) in the polar coordinate form:

$$\begin{aligned} \dot{r} &= \beta(\lambda)r + a(\lambda)r^3 + \cdots, \\ \dot{\theta} &= \omega(\lambda) + c(\lambda)r^2 + \cdots, \end{aligned} \tag{7.4}$$

then the Taylor expansion of (7.4) at $\lambda = \bar{\lambda}$ yields

$$\begin{aligned} \dot{r} &= \beta'(\bar{\lambda})(\lambda - \bar{\lambda})r + a(\bar{\lambda})r^3 + O(r|\lambda - \bar{\lambda}|^2, r^3|\lambda - \bar{\lambda}|, r^5), \\ \dot{\theta} &= \omega(\bar{\lambda}) + \omega'(\bar{\lambda})(\lambda - \bar{\lambda}) + c(\bar{\lambda})r^2 + O(|\lambda - \bar{\lambda}|^2, r^2|\lambda - \bar{\lambda}|, r^4). \end{aligned} \tag{7.5}$$

In order to determine the stability of the periodic solution, we need to calculate the sign of the coefficient $a(\lambda)$, which is given by

$$\begin{aligned} a(\bar{\lambda}) = &\frac{1}{16}[F^1_{xxx} + F^1_{xyy} + F^2_{xxy} + F^2_{yyy}] \\ &+ \frac{1}{16\omega(\bar{\lambda})}[F^1_{xy}(F^1_{xx} + F^1_{yy}) - F^2_{xy}(F^2_{xx} + F^2_{yy}) - F^1_{xx}F^2_{xx} + F^1_{yy}F^2_{yy}], \end{aligned}$$

where all partial derivatives are evaluated at the bifurcation point, i.e. $(x, y, \lambda) = (0, 0, \bar{\lambda})$.

Since y is linear in both $F^1(x, y, \lambda)$ and $F^2(x, y, \lambda)$, we have that

$$F^1_{xyy} = F^2_{yyy} = F^1_{yy} = F^2_{yy} \equiv 0.$$

At $(0, 0, \bar{\lambda})$, it is easy to calculate that

$$\begin{aligned} F^1_{xxx} + F^2_{xxy} &= 6A_{30} + 2B_{21} = 6(b_{30} - a_{30}) + 2a_{21}, \\ F^1_{xy}F^1_{xx} &= 2A_{11}A_{20} = -2(b_{20} - a_{20})a_{11}M_-, \\ F^2_{xy}F^2_{xx} &= 2B_{20}B_{11} = \frac{2}{M_-}a_{20}a_{11}, \\ F^1_{xx}F^2_{xx} &= 4A_{20}B_{20} = \frac{4}{M_-}a_{20}(b_{20} - a_{20}). \end{aligned}$$

Notice that

$$M^2_- = -\frac{C(\bar{\lambda})}{B(\bar{\lambda})} = \frac{f(\bar{\lambda})g'(\bar{\lambda})}{g(\bar{\lambda})}, \quad \text{and} \quad \omega(\bar{\lambda})M_- = C(\bar{\lambda}) = f(\bar{\lambda})g'(\bar{\lambda}).$$

By tedious but simple calculations, we obtain that

$$a(\bar{\lambda}) = \frac{H_1 + H_2}{16g'(\bar{\lambda})}, \tag{7.6}$$

where

$$\begin{aligned} H_1 &= [(fg)'''(\lambda) - g'''(\lambda)f(\lambda)]g'(\lambda)|_{\lambda=\bar{\lambda}}, \\ H_2 &= [g''(\lambda)f(\lambda) - (fg)''(\lambda)]\frac{[g'(\lambda)]^2 + g(\lambda)g''(\lambda)}{g(\lambda)}|_{\lambda=\bar{\lambda}}. \end{aligned} \tag{7.7}$$

Since $f'(\bar{\lambda}) = 0$, then (7.6) and (7.7) reduce to (3.3).

References

Aguirre P, González-Olivares E, Sáez E (2009) Three limit cycles in a Leslie-Gower predator-prey model with additive Allee effect. SIAM J Appl Math 69(5):1244–1262

Albrecht F, Gatzke H, Wax N (1973) Stable limit cycles in prey-predator populations. Science 181:1074–1075

Albrecht F, Gatzke H, Haddad A, Wax N (1974) The dynamics of two interacting populations. J Math Anal Appl 46:658–670

Allee WC (1931) Animal aggregations: a study in general sociology. University of Chicago Press

Alexander JC, Yorke JA (1978) Global bifurcations of periodic orbits. Am J Math 100:263–292

Arditi R, Ginzburg LR (1989) Coupling in predator-prey dynamics: ratio-dependence. J Theor Biol 139:311–326

Bazykin AD (1998) Nonlinear dynamics of interacting populations. World Scientific Series on nonlinear science. Series A: monographs and treatises, 11. World Scientific Publishing Co., Inc., River Edge

Berec L, Angulo E, Courchamp F (2007) Multiple Allee effects and population management. Trends Ecol Evol 22:185–191

Boukal SD, Berec L (2002) Single-species models of the Allee effect: extinction boundaries, sex ratios and mate encounters. J Theor Biol 218:375–394

Boukal SD, Sabelis WM, Berec L (2007) How predator functional responses and Allee effects in prey affect the paradox of enrichment and population collapses. Theor Popul Biol 72:136–147

Burgman MA, Ferson S, Akcakaya HR (1993) Risk assessment in conservation biology. Chapman and Hall, London

Cheng KS (1981) Uniqueness of a limit cycle for a predator-prey system. SIAM J Math Anal 12: 541–548
Chow SN, Mallet-Paret J (1978) The Fuller index and global Hopf bifurcation. J Differ Equ 29:66–85
Conway ED, Smoller JA (1986) Global analysis of a system of predator-prey equations. SIAM J Appl Math 46:630–642
Courchamp F, Clutton-Brock T, Grenfell B (1999) Inverse density dependence and the Allee effect. Trends Ecol Evol 14:405–410
Courchamp F, Berec L, Gascoigne J (2008) Allee effects in ecology and conservation. Oxford University Press, Oxford
Dennis B (1989) Allee effect: population growth, critical density, and chance of extinction. Nat Resour Model 3:481–538
Dhooge A, Govaerts W, Kuznetsov YA (2003) MATCONT: a MATLAB package for numerical bifurcation analysis of ODEs. ACM Trans Math Softw 29:141–164
Edelstein KL (1998) Mathematical models in biology. Random House, New York
Gascoigne JC, Lipcius RN (2004) Allee effects driven by predation. J Appl Ecol 41:801–810
González-Olivares E, González-Yaez B, Sáez E, Szántó I (2006) On the number of limit cycles in a predator prey model with non-monotonic functional response. Discrete Contin Dyn Syst B 6(3):525–534
Gruntfest Y, Arditi R, Dombrovsky Y (1997) A fragmented population in a varying environment. J Theor Biol 185:539–547
Hassard BD, Kazarinoff ND, Wan Y (1981) Theory and applications of Hopf bifurcation. London Math Soc Lecture Note Ser, vol 41. Cambridge University Press, Cambridge
Hilker FM, Langlais M, Malchow H (2009) The Allee effect and infectious diseases: extinction, multistability, and the (dis-)appearance of oscillations. Am Nat 173:72–88
Holling CS (1959) The components of predation as revealed by a study of small mammal predation of the European Pine Sawfly. Can Entomol 91:293–320
Hsu SB (1978) On global stability of a predator-prey system. Math Biosci 39:1–10
Hsu SB (2006) Ordinary differential equations with applications. Series on Applied Mathematics, vol 16. World Scientific Publishing Co., Hackensack
Hsu SB, Shi J (2009) Relaxation oscillator profile of limit cycle in predator-prey system. Discrete Contin Dyn Syst B 11(4):893–911
Hsu SB, Hwang TW, Kuang Y (2001) Global analysis of the Michaelis-Menten-type ratio-dependent predator-prey system. J Math Biol 42:489–506
Ivlev VS (1955) Experimental ecology of the feeding of fishes. Yale University Press
Jacobs J (1984) Cooperation, optimal density and low density thresholds: yet another modification of the logistic model. Oecologia 64:389–395
Jiang J, Shi J (2009) Bistability dynamics in some structured ecological models. In: Spatial ecology. CRC Press, Boca Raton
Kazarinov N, van den Driessche P (1978) A model predator-prey systems with functional response. Math Biosci 39:125–134
Kuang Y, Beretta E (1998) Global qualitative analysis of a ratio-dependent predator-prey system. J Math Biol 36:389–406
Kuang Y, Freedman HI (1988) Uniqueness of limit cycles in Gause-type models of predator-prey systems. Math Biosci 88:67–84
Kuznetsov YA (2004) Elements of applied bifurcation theory. Appl Math Sci, vol 112. Springer-Verlag, New York
Lande R (1987) Extinction thresholds in demographic models of territorial populations. Am Nat 130:624–635
Lewis MA, Kareiva P (1993) Allee dynamics and the spread of invading organisms. Theor Popul Biol 43:141–158
Lotka AJ (1925) Elements of physical biology. Williams and Wilkins, Baltimore
Malchow H, Petrovskii SV, Venturino E (2008) Spatiotemporal patterns in ecology and epidemiology. Theory, models, and simulation. Chapman & Hall/CRC Mathematical and Computational Biology Series. Chapman & Hall, Boca Raton
May RM (1972) Limit cycles in predator-prey communities. Science 177:900–902
Morozov A, Petrovskii S, Li B-L (2004) Bifurcations and chaos in a predator-prey system with the Allee effect. Proc R Soc Lond B Biol Sci 271:1407–1414

Morozov A, Petrovskii S, Li B-L (2006) Spatiotemporal complexity of patchy invasion in a predator-prey system with the Allee effect. J Theor Biol 238(1):18–35
Owen MR, Lewis MA (2001) How predation can slow, stop or reverse a prey invasion. Bull Math Biol 63:655–684
Petrovskii SV, Morozov A, Venturino E (2002) Allee effect makes possible patchy invasion in a predator-prey system. Ecol Lett 5:345–352
Petrovskii S, Morozov A, Li B-L (2005) Regimes of biological invasion in a predator-prey system with the Allee effect. Bull Math Biol 67(3):637–661
Polking JA, Arnold D (2003) Ordinary differential equations using MATLAB, 3rd edn. Prentice-Hall, Englewood Cliffs
Rosenzweig ML (1969) Why the prey curve has a hump? Am Nat 103:81–87
Rosenzweig LM (1971) Paradox of enrichment: destabilization of exploitation ecosystems in ecological time. Science 171(3969):385–387
Rosenzweig ML, MacArthur R (1963) Graphical representation and stability conditions of predator-prey interactions. Am Nat 97:209–223
Ruan S, Xiao D (2000) Global analysis in a predator-prey system with nonmonotonic functional response. SIAM J Appl Math 61:1445–1472
Shi J, Shivaji R (2006) Persistence in reaction diffusion models with weak Allee effect. J Math Biol 52:807–829
Stephens PA, Sutherland WJ (1999) Consequences of the Allee effect for behaviour, ecology and conservation. Trends Ecol Evol 14:401–405
Stephens PA, Sutherland WJ, Freckleton RP (1999) What is the Allee effect? Oikos 87:185–190
Takeuchi Y (1996) Global dynamical properties of Lotka-Volterra systems. World Scientific, Singapore
Thieme HR, Dhirasakdanon T, Han Z, Trevino R (2009) Species decline and extinction: synergy of infectious disease and Allee effect? J Biol Dyn 3:305–323
Turchin P (2003) Complex population dynamics: a theoretical/empirical synthesis. Princeton University Press
van Voorn GAK, Hemerik L, Boer MP, Kooi BW (2007) Heteroclinic orbits indicate overexploitation in predator prey systems with a strong Allee effect. Math Biosci 209:451–469
Volterra V (1926) Fluctuations in the abundance of species, considered mathmatically. Nature 118:558
Wang ME, Kot M (2001) Speeds of invasion in a model with strong or weak Allee effects. Math Biosci 171:83–97
Wiggins S (1990) Introduction to applied nonlinear dynamical systems and chaos. Texts Appl Math, vol 2. Springer, New York
Wilson EO, Bossert WH (1971) A primer of population biology. Sinauer Assoxiates, Sunderland
Wu J (1998) Symmetric functional-differential equations and neural networks with memory. Trans Am Math Soc 350:4799–4838
Xiao D, Ruan S (2001) Global dynamics of a ratio-dependent predator-prey system. J Math Biol 43:268–290
Xiao D, Zhang Z (2003) On the uniqueness and nonexistence of limit cycles for predator-prey system. Nonlinearity 16:1–17
Xiao D, Zhang Z (2008) On the existence and uniqueness of limit cycles for generalized Liénard systems. J Math Anal Appl 343:299–309
Zeng X, Zhang Z, Gao S (1994) On the uniqueness of the limit cycle of the generalized Liénard equation. Bull Lond Math Soc 26:213–247
Zhang ZF (1986) Proof of the uniqueness theorem of limit cycles of generalized Liénard equations. Appl Anal 23(1–2):63–76
Zhou SR, Liu YF, Wang G (2005) The stability of predator-prey systems subject to the Allee effects. Theor Popul Biol 67(1):23–31